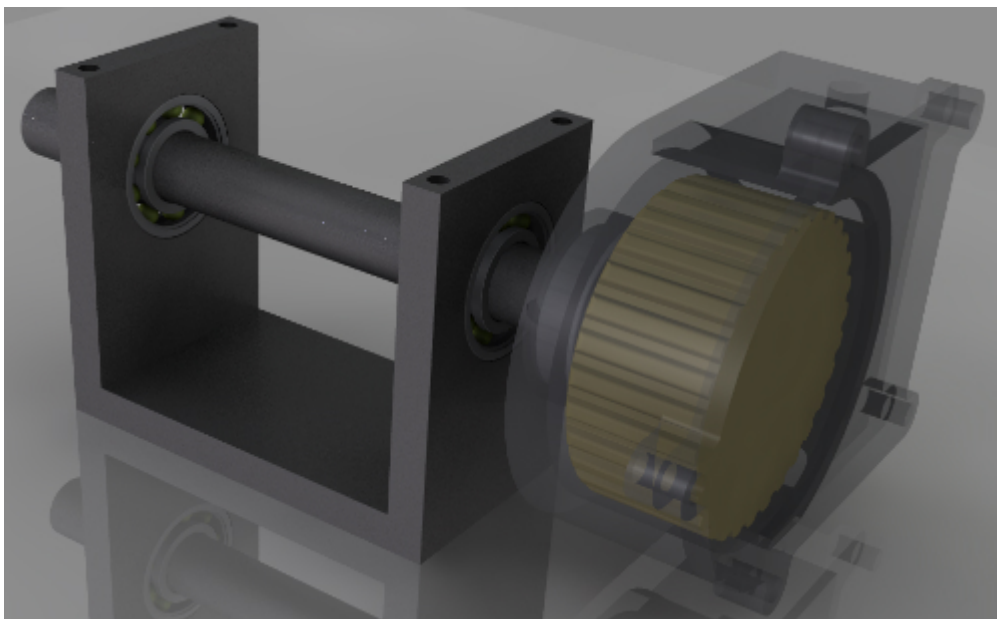


Predicting drag losses & oil flow characteristics in a wet clutch system using numerical analysis



Marcus Liljegren
Edin Ljeskovica

**Mechanical Engineering, masters level
2016**

Luleå University of Technology
Department of Engineering Sciences and Mathematics

PREDICTING DRAG LOSSES & OIL FLOW CHARACTERISTICS IN A WET CLUTCH
SYSTEM USING NUMERICAL ANALYSIS

A MASTER'S THESIS STUDY

BY

MARCUS LILJEGREN

EDIN LJESKOVICA

Abstract

This report presents the Master Thesis done by two students at the Mechanical Engineering program, Machine Design at Luleå University of Technology. The thesis was performed at Luleå University of Technology in collaboration with BorgWarner PDS located in Landskrona. The objective for the thesis was to study the potential for predicting and optimizing drag losses and oil flow characteristics in a wet clutch system using numerical simulations in LS-DYNA.

BorgWarner PDS manufactures and distributes the Haldex coupling, which is an electro-hydraulic coupling used in an active four-wheel drive system. BorgWarner PDS strives to make the Haldex coupling more efficient by minimizing energy losses in order to lower fuel consumption for the vehicle and a smaller impact on the environment. As testing on prototypes are costly and time consuming it is therefore desirable to use numerical simulations instead.

To determine the potential for numerical simulations to predict and optimize both drag losses and oil flow characteristics a numerical model was set up using LS-DYNA. A test rig was designed in order to achieve a controlled testing environment in order to validate the numerical models, both qualitatively and quantitatively. The numerical model uses the built in Fluid Structure Interaction method in LS-DYNA, which is a combination of a structural model and an incompressible fluid model.

The test rig measures torque on the clutch housing induced by the dragging of oil as the clutch drum rotates. The tests were performed using different rotational speeds, varying from 250-1500 rpm, and different clutch housing geometries. The results were gathered from an average of ten measurements of the drag torque. A high-speed camera was also used to capture the oil flow characteristics. The numerical simulations were done using the same parameters used for the tests i.e. different rotational speeds and clutch housing geometries. In addition, each simulation was performed using different mesh sizes; 0.5 mm, 1 mm and 2 mm in order to analyze mesh dependence. The numerical model was set to measure the drag torque on the clutch drum and was then compared to the experimental results in order to validate the numerical model quantitatively. The oil flow characteristics from the numerical simulation were compared to the high-speed movies to validate the numerical model qualitatively.

The numerical model shows promising results when it comes to predicting drag torque and oil flow characteristics. The results also show that using a numerical model for optimization purposes are possible as the experimentally measured drag torque at different clutch house geometries corresponds to the numerically simulated drag torque.

The conclusions from this Master Thesis is that numerical simulations do have a potential for predicting drag losses and oil flow characteristics in a wet clutch system. The numerical model created in this project can also be used to obtain valuable information about geometry changes when it comes to optimizing the wet clutch system. However, the numerical model is still at an early stage and can be seen as a second generation model where further work needs to be done in order to include more of the complex geometries of a wet clutch system have. Although LS-DYNA is state-of-the-art when it comes to these kinds of complex simulations it still needs to be developed further to handle such complex simulations.

Acknowledgements

First of all, we want to thank our supervisors Pär Jonsén and Pär Marklund at Luleå University of Technology and Kathiravan Ramanujam at BorgWarner PDS for great collaboration and guidance throughout the thesis work. Without you, this thesis would not have been possible! We also want to thank BorgWarner for the financing and the opportunity to do this thesis work. It has been a lot of fun and we have learned a lot,
thank you!

We would also like to thank Erik Söderström for his early involvement in the project by laying the foundation which led to this thesis work and for his guidance. Special thanks go to Tore Serrander for his guidance, but most importantly by providing us with materials throughout the thesis work. Without your contributions we would have spent a lot of time going back and forth to the hardware store buying epoxy, etc. Also, a big thanks goes to Tore Silver for support in the workshop and to Pär Gren for the usage of the high-speed camera.

There are many more people we would like to thank, especially our families, for the support and guidance to achieve this Master's degree. To all of you that were involved in this thesis,
Thank You it means the world to us!

Table of Contents

1. Introduction	7
1.1. Wet Clutch System	8
1.2. Drag Torque in Wet Clutch Systems	8
1.3. FSI Simulations in LS-DYNA	9
1.4. Earlier Work	9
1.5. Objectives	10
1.6. Thesis Statement & Delimitations	10
2. Theory	12
2.1. Tribological losses	12
2.1.1. Drag losses in a wet clutch	12
2.2. The Fluid/Structure Interaction (FSI)	14
2.3. Fluid domain	15
2.3.1. ICFD solver	15
2.3.2. ICFD Volume mesh.....	18
2.3.3. Lagrangian description	20
2.3.4. Eulerian description.....	21
2.3.5. Arbitrary Lagrangian-Eulerian Description (ALE)	21
2.3.6. Level set method	22
2.4. Structure domain	24
2.4.1. Mesh.....	24
3. Method.....	26
3.1. Design of Experimental Setup.....	26
3.1.1. Conceptual Design Aspects.....	26
3.1.2. CAD-model of Conceptual Design Aspects	29
3.1.3. Volume Verification of Wet Clutch Housing	37
3.1.4. Structural Analysis of Test Setup	37
3.2. Numerical Model	38
3.2.1. Model structure.....	38
3.2.2. Geometry & Meshing	39
3.2.3. Model Setup	42
3.2.4. Simulation.....	43
3.3. Experiments	43

3.3.1.	Experimental Setup	44
3.3.2.	Experimental Procedure	45
3.3.3.	Preparation of data.....	46
3.4.	Validation of Numerical Model.....	47
3.4.1.	Drag Torque.....	47
3.4.2.	Oil Flow Characteristics	47
3.4.3.	Oil Entering the Oil Sump	47
4.	Results	48
4.1.	Experimental Results	48
4.2.	Model Validation, 2.5 mm inlet	49
4.3.	Model Validation, 10 mm inlet	50
4.4.	Mesh Study	51
4.5.	Geometry Dependent Drag Torque Losses	52
4.6.	Oil Flow Characteristics.....	54
5.	Discussion.....	57
5.1.	Experimental Setup.....	57
5.2.	Numerical Model vs. Experimental Setup.....	57
5.3.	Mesh Study	58
5.4.	Geometry Dependent Drag Torque Losses	58
5.5.	Oil Flow Characteristics.....	58
6.	Conclusions	60
7.	Future work.....	61
8.	References.....	62

1. Introduction

As the environmental issues grow larger and larger, companies worldwide are developing more eco-friendly solutions that will leave a smaller imprint on the environment. Companies producing consumable products e.g. food containers, the paper industry and the cell phone industry are focusing on developing new eco-friendly materials. They benefit from this by the way consumers see and think about the company and the product. The automotive industry is focusing on finding ways to reduce fuel consumption and minimizing CO₂ pollution by developing components with reduced energy losses and also by changing the choice of fuel used in the vehicle. The benefits are clear to both consumer and the environment as lower energy losses translate to lower fuel consumption that will lower the cost of the fuel needed to operate the vehicle [1].

This thesis work focuses on the energy losses found in vehicle power trains, more specifically the wet clutches situated in All-Wheel Drive (AWD) couplings. As friction in the engine, transmission, tires and brakes stands for almost one third of the total fuel energy and only around 21 % of the fuel energy is used to actually move the vehicle [2], companies must continuously optimize components of the power train in order to minimize these energy losses. The energy losses in a wet clutch are mainly due to shearing, splashing and churning of the oil inside the clutch [3]. These energy losses result in a drag torque, which counteract the applied torque from the driven shaft.

Experiments can be done to determine the drag torque of a wet clutch system as well as the oil flow characteristics inside the housing. These measurements can then be used to analyze and optimize the wet clutch system in order to minimize the drag torque. However, although it is possible to measure drag torque, it is not very efficient as the process is time consuming and expensive. For these measurements to be successful, prototypes of different types of wet clutch systems needs to be designed and manufactured and the test setup is not versatile enough to be profitable as direct optimizations on the prototype are not always possible.

A faster and less expensive way to optimize and analyze the system is by a numerical simulation approach. Numerical simulations have advanced a lot when it comes to structural analysis and is widely used in construction optimization, product development and analysis. Numerical structural analysis is much faster and much less expensive than experimental analysis and provides a good prediction of the real scenario. The possibility to predict deformations, load, pressure etc. in a shorter time than for experimental analysis leads to a faster optimization and changes to geometries without the need to reproduce any prototypes. A challenge, when it comes to numerical simulation of fluid flow, although widely used in the automotive and aerospace industries, it is not as accurate when it comes to Fluid Structure Interaction (FSI) as the complexity of the model and numerical tools have not been developed to the same extent as for structural and fluid analysis separately.

1.1. Wet Clutch System

“A wet clutch is a mechanical device that transmits power from input member to output member through frictional and viscous effects.” [4]

A wet clutch can be found in many different setups such as in automatic transmissions, limited slip differentials and wet brakes. BorgWarner PDS, who is one of the biggest manufacturers of limited slip differentials, manufactures the Haldex Limited Slip Coupling (LSC) which is an AWD system used in the Volkswagen Group and Volvo Cars among others. The AWD system manufactured and developed by BorgWarner is an active four-wheel drive system that mainly uses Forward Wheel Drive (FWD) or in some cases Rear Wheel Drive (RWD). A control system is controlling the Haldex LSC, which activates the AWD when there is a difference in rotational speed between the front wheels and the rear wheels [5]. The Haldex LSC

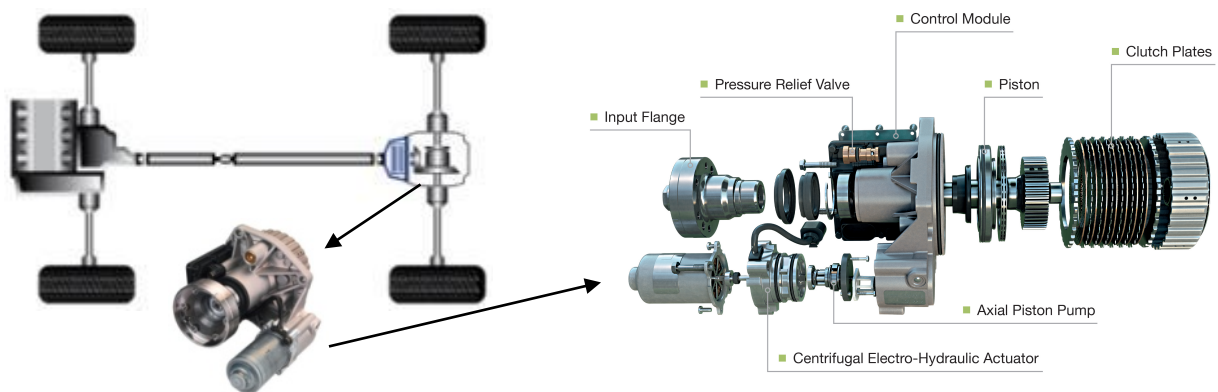


Figure 1.1. Haldex LSC GenV on power train (left), exploded view of Haldex LSC GenV (right). [5]

GenV (generation 5) is illustrated in Figure 1.1 below.

The AWD system can manage to distribute 96% of the total torque from the front wheel axis to the rear wheel axis and alter in between [6]. The benefits from this setup is that the vehicle does not always drive on four-wheel drive but instead uses either FWD or RWD until the wheels loses traction and the AWD is activated. This ensures a lower flue consumption as the vehicle only uses four-wheel drive when it is necessary. However, as the clutch is not engaged the clutch drum will still rotate inside the wet clutch housing generating energy losses in the form of drag torque.

1.2. Drag Torque in Wet Clutch Systems

In a wet clutch system, the clutch drum will always experience a drag that counteracts the rotational torque. This energy loss is called drag torque and comprises churning, windage and shearing. Churning and shearing is due to the oil inside the clutch housing and stands for most of the drag torque at lower rotational speeds. Shearing of the oil takes place inside the clutch drum in between the frictional and separator discs when the clutch is disengaged. However, shearing does not have great affect when the difference in rotational speed inside the clutch is low. Churning takes place as the clutch drum rotates partly submerged in oil and splashes the oil inside the housing. Windage only inflicts a significant energy loss at higher rotational speeds (above 5000 rpm) and is caused by the air surrounding the rotating clutch drum.

The drag torque is mainly dependent of the following [7]:

- Geometry of clutch housing and clutch drum
- Immersion depth and surface area of the clutch drum
- Rotational speed
- Viscosity and density of the oil

1.3. FSI Simulations in LS-DYNA

Since the release of LS-DYNA v.970 R7 a multi-physics solver, combining both fluid dynamics and structural solvers, was introduced. This multi-physics solver is capable of handling both incompressible and compressible fluid dynamic problems while integrated with a solid mechanic problem allowing for fluid structure interaction problems to be analyzed. This shows a promising and powerful design tool for the aerospace and automotive industry [8]. Since the first release of the multi-physics solver, further development has been done to the most recent LS-DYNA R8.1.0 solver, where faster and more stable FSI problem calculations are promised. Further development has also been done on the incompressible fluid dynamic (ICFD) solver. The potential for these kinds of problems are truly promising and Dynamore and Lawrence Livermore National Laboratory, the companies behind LS-DYNA, continuously develops the solvers.

1.4. Earlier Work

It has been shown that the possibility to predict both drag torque and oil flow characteristics in a wet clutch is accurate to a relevant degree. Earlier work consists of both 2D- and 3D-models of wet clutch systems for investigating the capability to handle FSI problems using the ICFD solver in LS-DYNA [9] [10]. Both model studies are simplified as they are said to be first generation simulation models and further work was needed in order to develop a second generation, which will further on be developed closer to engineering applications. In order to develop second generation simulation models the following conclusions was mentioned in earlier work:

- Design of a better test setup used to validate the models
- Investigate the effect of viscous drag
- Investigate the effect of windage (drag torque induced by air)
- Making the FSI numerically stable for the 3D-model
- Adding an oil sump to the wet clutch model in order to mimic a wet clutch better
- Do a more comprehensive mesh study

Although earlier work showed promising results, it is still a challenge to virtually reproduce all phenomena in an engineering application of a wet clutch system [10].

1.5. Objectives

The main objective of this thesis work is to investigate if it is possible to build physically realistic models and predict the drag torque and oil flow characteristics of a wet clutch. A second objective is to evaluate how well the numerical model can predict an actual case by validating the numerical model against experimental quantitative results from a real case.

1.6. Thesis Statement & Delimitations

Like the previous work done the numerical model will be set up using LS-DYNA, this time with the further developed solver R 8.1.0. The new solver promises faster and more stable simulations for FSI problems as earlier solvers were not developed to the same extent when it comes to FSI problems. Following work will be done on the numerical models:

- Adding an oil sump and evaluating the oil flow characteristics
- Complete redesign of CAD models used in both numerical simulations to mimic the new test setup
- Structuring the numerical model to make them more implementable on different wet clutch housings
- Making a numerically stable 3D-model with and without FSI-coupling
- Comparing the 2D- and 3D-models against each other in terms of reliability and simulation capabilities
- Investigate the possibilities of optimization using the 2D-model
- Validating the models using a new test setup

As earlier work states that this type of multi-physics simulation is very complex it is necessary to set up delimitations to the numerical models. These will include:

- Thermal effects will be neglected
- Shearing between the lamellae will not be investigated as the clutch drum will be fully enclosed
- Air inside the wet clutch housing will be modeled as void
- Simplify the geometry of the oil sump as much as possible
- The main focus should be on the 3D-model
- Optimization of wet clutch housing will only be performed on the 2D-model

Furthermore, a new test setup will be designed to make for more stable measurements and more accurate readings of data. Following work will be done on the test setup:

- Design of new test setup including the oil sump
 - Focus on simplicity of the design to meet the requirements set by the numerical model
 - Focus on versatility of the test setup
 - Use of an electric motor easily controlled with speed and acceleration
- Manufacturing of new test setup
- Investigation of possible measurement tools

Delimitations regarding the test setup will include:

- The manufacturing of the new wet clutch housing will be outsourced to a suitable manufacturing company
- Thermal effects will not be investigated and all measurements will be designed for and performed in room temperature
- The main focus should be on the wet clutch housing and measurement tools
- The design of the wet clutch housing will only be suitable for experimental purposes

2. Theory

2.1. Tribological losses

Tribology is the study of surface interaction in relative motion and also includes lubricants, wear and friction. Tribology often also refers to the behavior of the active media in between the interacting surfaces [11]. Tribological losses can be found virtually anywhere where there are surfaces in relative motion in the form of friction or wear. In a wet clutch the main tribological losses are represented by friction in between the lamellae and viscous friction e.g. drag induced by the rotating clutch drum being partly submerged in oil. As this thesis work focuses on calculation of the drag losses the friction losses will thereby not be investigated.

2.1.1. Drag losses in a wet clutch

The drag losses in a wet clutch are caused by solid surfaces interacting with an active media in relative motion. To make this easier to grasp the solid surfaces are the inner walls of the clutch housing and the clutch drum and the active medium is the oil in which the clutch drum is partly submerged in and the air inside the housing. As the clutch housing can be seen as fixed the surfaces interact in relative motion as the clutch drum continuously rotates at different rotational speeds in relation to the housing. The clutch drum is partly submerged in oil and surrounded by air that acts like a link between the drum and walls. A schematic 2D-representation of this can be seen in Figure 2.1 below.

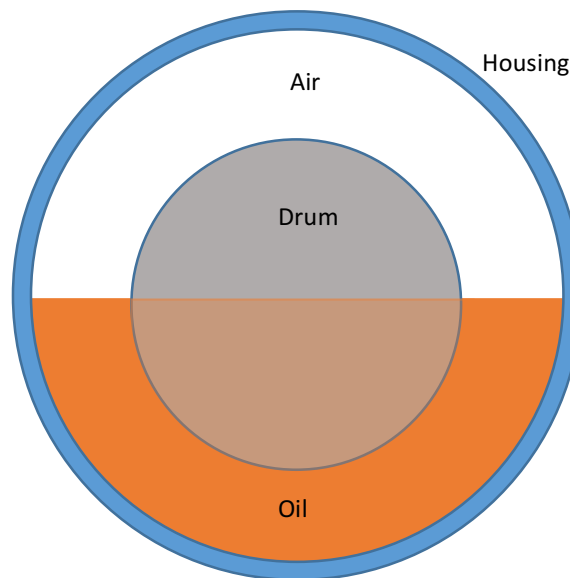


Figure 2.1. Schematic 2D-representation of simplified wet clutch

The total drag loss in the wet clutch system can be divided into two different losses, namely drag loss caused by the oil and drag loss caused by the air.

Churning losses

The drag loss caused by the oil can also be called churning losses which is commonly studied among gears and transmissions. Churning gives rise to energy losses, which increase as the oil immersion depth increase. The energy losses increase even further as the rotational speed increases. This is due to the fact that the oil is being dragged and splashed more aggressively inside the clutch housing. Viscosity also affects the power loss, higher viscosity mediums tend to increase the energy loss and vice versa [12]. The clutch housing dimensions also play a role in the energy loss caused by churning. If the axial clearance between the clutch drum and housing walls is decreased the churning effects will be larger and result in an increase of energy loss. The radial clearance however does not have an effect on churning losses [7].

Windage losses

The drag loss caused by windage only becomes important when the rotational speeds are very high (above 5000 rpm). This has to do with the medium being in a laminar state or a turbulent state. When the medium transitions into the turbulent state the interaction between the medium and, in this case, the clutch drum becomes more aggressive and vortexes forms. This result in an increase of windage losses as the relative motion between the drum and the air causes larger and larger air resistance [13]. The windage power loss (WPL) from a gear wheel rotating in a closed housing with a 5mm radial clearance gap can be seen in Figure 2.2.

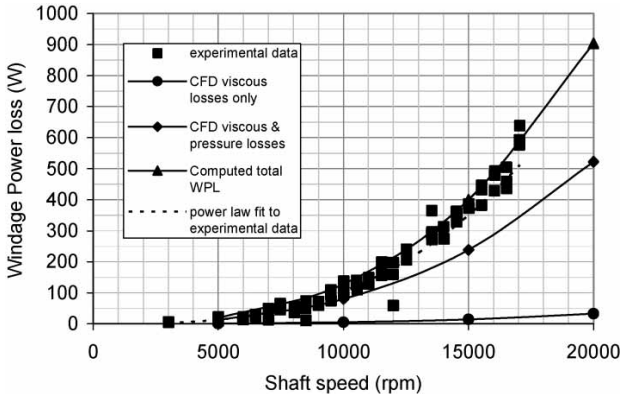


Figure 2.2. Windage Power loss (WPL) in relation to shaft speed (rpm) [13]

However, wet clutch systems used in personal vehicles not often reach more than 3000 rpm.

2.2. The Fluid/Structure Interaction (FSI)

The FSI is used when a Structure is interacting with a Fluid. The FSI consist of two separate domains, one structural domain and one fluid domain. The domains are connected at an interface where information is transferred between the solvers as output and input data, while the solvers solve the problems independently. The FSI starts with the Structure domain and implicitly solves the first time step for the given initial conditions and gives output in form of displacement and velocity. The output parameters are used as input parameters for the fluid solver due to the interface between the structure and fluid. The fluid solver implicitly solves for the forces and checks for convergence. If it does not converge the iteration process starts until convergence is achieved and next time step can be calculated, see Figure 2.3. This type of FSI coupling is also known as strong two way FSI coupling while one way FSI coupling only sends information in one direction, either form the structure to the fluid or from the fluid to the structure [14].

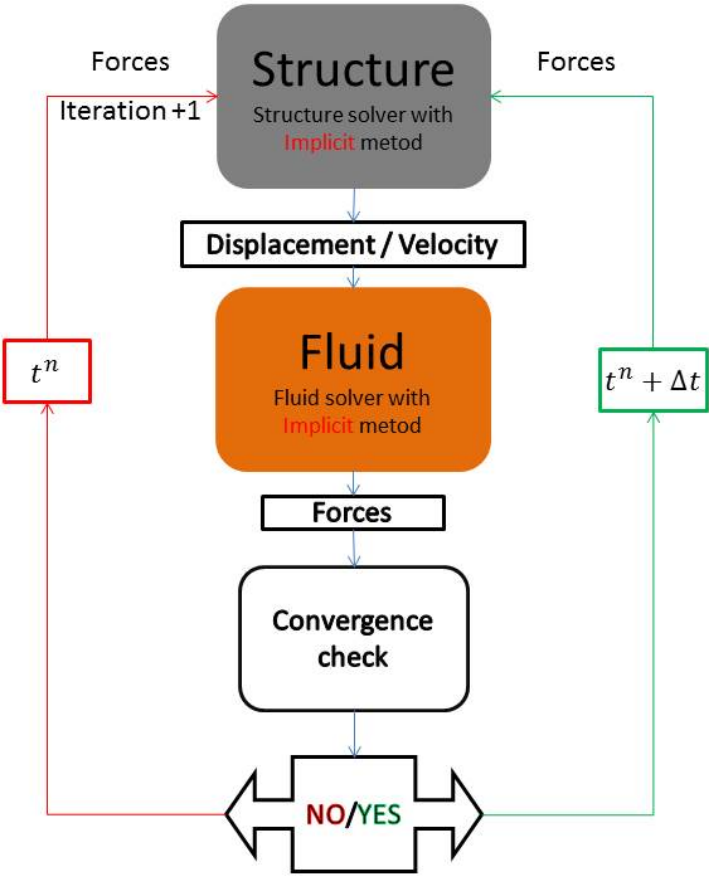


Figure 2.3. FSI communication between the Fluid and Structure.

2.3. Fluid domain

The fluid domain is solved with the ICFD solver in LS-DYNA which automatically meshes the volume for the fluid domain. The solver uses two types of numerical approaches, the Lagrangian and the Eulerian due to the FSI coupling and is also known as the arbitrary Lagrangian Eulerian approach (ALE). The Lagrangian approach is used in at the interface between the fluid and structure while the Eulerian is used in the volume of the fluid, see Figure 2.4. The fluid domain also consists of a level set method to set boundaries between different fluids.

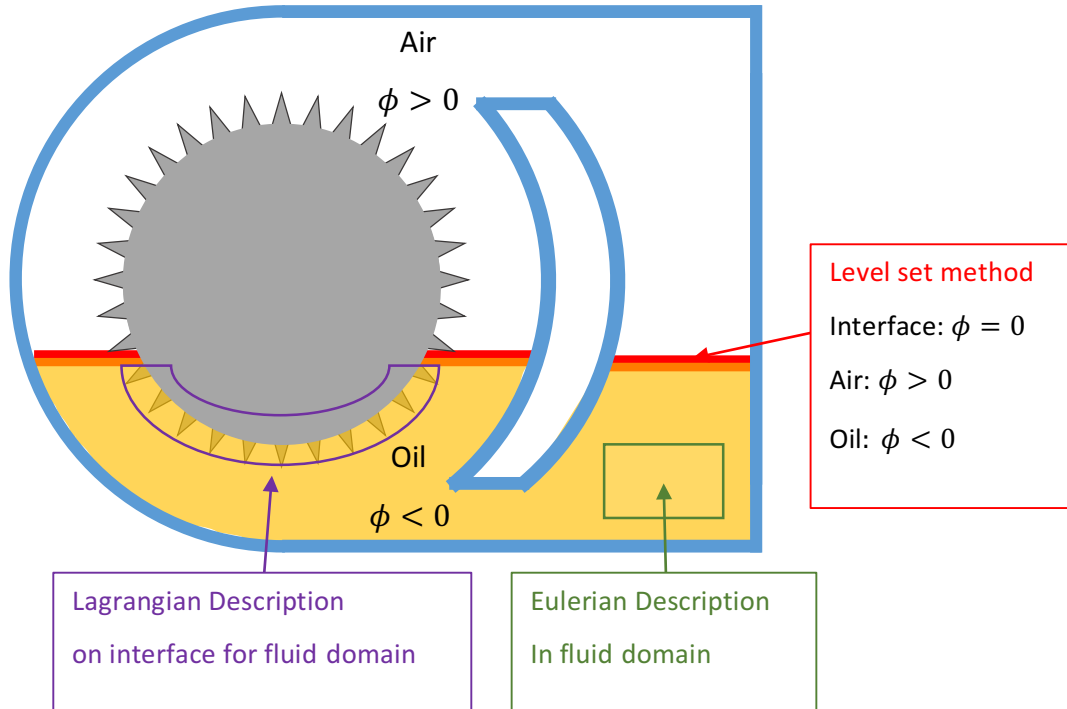


Figure 2.4. Lagrangian, Eulerian and level set method illustrated.

2.3.1. ICFD solver

The incompressibility condition

The LS-DYNA solver is solving the incompressible Navier-Stokes equations. A fluid with Mach number lower than 0.3 is considered as an incompressible fluid. Calculation of the Mach number according to

$$M = \frac{V}{a} \leq 0.3, \quad (2.1)$$

where M is the Mach number, V is the velocity of the fluid relative to a fixed object and a is the speed of sound in the medium. The solver is based on a continuity equation that states that all mass entering the system must equal the mass leaving the system at a steady state process.

The continuity equation can be written as (2.2)

$$\frac{\partial \rho}{\partial t} + \nabla \cdot (\rho \vec{u}) = 0, \quad (2.2)$$

where ρ is the density, t is the time and \vec{u} is the velocity.

The continuity equation can be simplified to a volume continuity equation

$$\nabla \cdot \vec{u} = 0, \quad (2.3)$$

due to the fact that the fluid is incompressible which means that the ρ is constant.

Governing set of equations

A combination of the continuity equation and Navier-Stokes equations as seen below is an incompressible Newtonian fluid in an Eulerian conventional form, where mass and momentum are conserved.

$$\rho \left(\frac{du_i}{dt} + u_j \frac{\partial u_i}{\partial x_j} \right) = \frac{\partial \sigma_{ij}}{\partial x_j} + \rho f_i, \quad \text{in } \Omega, \quad (2.4)$$

where Ω is a closed volume, f_i are the forces applied, usually gravity, u_i is the flow velocity and σ_{ij} is the total stress tensor.

$$\frac{\partial u_i}{\partial x_i} = 0, \quad \text{in } \Omega. \quad (2.5)$$

The total stress tensor, σ_{ij}

$$\sigma_{ij} = -p\delta_{ij} + \mu \left(\frac{\partial u_i}{\partial x_j} + \frac{\partial u_j}{\partial x_i} - \frac{2}{3} \frac{\partial u_l}{\partial x_l} \delta_{ij} \right), \quad (2.6)$$

where p is the pressure, μ is the dynamic viscosity and δ_{ij} is the Kronecker delta which is

$$\delta_{ij} = \begin{cases} 1 & i = j \\ 0 & i \neq j \end{cases} \quad (2.7)$$

Because of incompressible flow we have that

$$\frac{\partial u_l}{\partial x_l} \ll \frac{\partial u_i}{\partial x_j}, \quad (2.8)$$

which means that the last term in (2.6) can be neglected as following

$$\sigma_{ij} \approx -p\delta_{ij} + \mu \left(\frac{\partial u_i}{\partial x_j} + \frac{\partial u_j}{\partial x_i} \right). \quad (2.9)$$

This also means that $\frac{\partial \sigma_{ij}}{\partial x_j}$ in the momentum equation can be simplified due to incompressible flow as following,

$$\begin{aligned} \frac{\partial \sigma_{ij}}{\partial x_j} &= -\frac{\partial p}{\partial x_j} \delta_{ij} + \frac{\partial}{\partial x_j} \left[\mu \left(\frac{\partial u_i}{\partial x_j} + \frac{\partial u_j}{\partial x_i} \right) \right] \\ &= -\frac{\partial p}{\partial x_j} \delta_{ij} + \mu \frac{\partial}{\partial x_j} \left(\frac{\partial u_i}{\partial x_j} \right) + \mu \frac{\partial}{\partial x_j} \left(\frac{\partial u_j}{\partial x_i} \right) \\ &= -\frac{\partial p}{\partial x_j} \delta_{ij} + \mu \frac{\partial}{\partial x_j} \left(\frac{\partial u_i}{\partial x_j} \right) + \mu \frac{\partial}{\partial x_i} \left(\frac{\partial u_j}{\partial x_j} \right) \\ &\approx -\frac{\partial p}{\partial x_j} \delta_{ij} + \mu \frac{\partial}{\partial x_j} \left(\frac{\partial u_i}{\partial x_j} \right). \end{aligned} \quad (2.10)$$

By using the simplified momentum equation (2.10) into (2.4), is following system obtained

$$\rho \left(\frac{du_i}{dt} + u_j \frac{\partial u_i}{\partial x_j} \right) = -\frac{\partial p}{\partial x_i} + \mu \frac{\partial^2 u_i}{\partial x_j \partial x_j} + \rho f_i, \quad (2.11)$$

$$\frac{\partial u_i}{\partial x_i} = 0. \quad (2.12)$$

The set of equations are incomplete without proper boundary conditions and initial conditions, which will be further introduced.

Boundary conditions and initial conditions

To make the set of equations above complete, some proper initial conditions have to be specified. Velocities and stress have to be defined for the continuum problem. The velocity vector will be redefined with new values due to the constraint on the boundary. When free-slip conditions are used on a wall then the normal velocity must be zero and for non-slip conditions the tangential components have to be same velocity as the wall and still have a zero normal velocity, a generalization of the conditions is

$$u_i = \bar{v}_i \text{ on } \Gamma_v, \quad (2.13)$$

where \bar{v}_i is the funktion imposed on the boundary Γ [14].

The second boundary condition has to be computed ahead, which makes it more difficult to identify and it is used on the free surface. To fulfill the free surface conditions, the stress, tangential to the surface must disappear and the normal of the surface must balance the external applied normal stresses and is expressed as following,

$$t_i = \sigma_{ij}n_j = \bar{t}_i \text{ on } \Gamma_f. \quad (2.14)$$

For the Lagrangian Navier-Stokes problem, the initial conditions will be set by specifying the pressure and velocity at the initial time

$$v_i(x_i, 0) = v_i^0(x_i), \quad (2.15)$$

$$p(x_i, 0) = p^0(x_i), \quad (2.16)$$

where v_i^0 is the initial velocity and p^0 is the initial pressure. v_i^0 needs to satisfy the incompressibility constrain [14].

2.3.2. ICFD Volume mesh

As mentioned earlier the ICFD automatically meshes the volume which simplifies the preprocessing in LS-DYNA and in case of large deformations due to the FSI coupling the solver can automatically re-mesh to improve the mesh quality. In this section an explanation will be given about the basics in how LS-DYNA creates the mesh and computes the re-meshing [14].

The Delaunay criteria

To obtain better understanding of the meshing the solver computes, a fundamental constrain has to be introduced, called the Delaunay criteria. The Delaunay criteria is a type of triangulation for a set of nodes P also known as $DT(P)$. The criterion is that any three points that combines into a triangle also have a circumcircle around the point and no other point can be placed inside the circle. As shown to the left in Figure 2.5 the points P_1 , P_2 and P_3 creates a triangular element with a circumcircle shown in black and because P_4 is inside this circumcircle the criteria is not fulfilled. On the right side of Figure 2.5 a fulfilled criterion is shown where P_4 is outside the circumcircle. The Delaunay criteria establishes good geometrical angels for the triangular elements by preventing to small or to large angels which leads to a reliable automatic created fluid mesh [14].

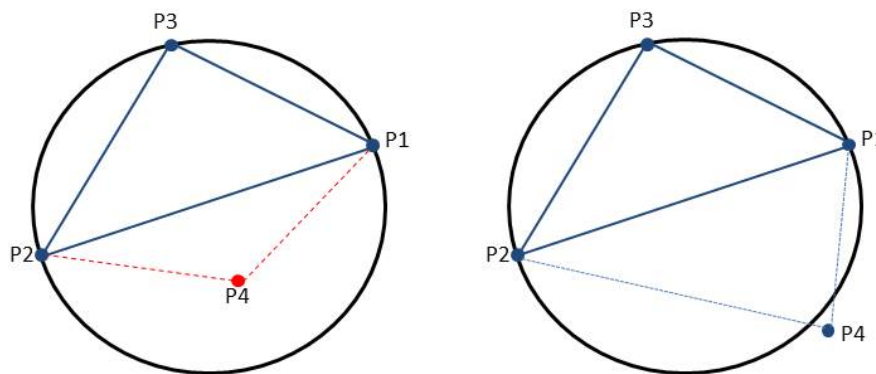


Figure 2.5. The Delaunay criteria, the left circle dose not fulfill the criteria while the right one does [14].

Mesh building steps

The creation of the fluid mesh can be summarized in three steps.

- First of all, the user has to define the nodes and elements that are going to be used to create the mesh which can is shown in Figure 2.6. This can be shell elements in regards to 3D modelling and beam elements in regards to 2D simulations. During this step some important demands have to be met, if they are not met an error will occur [14].
 - The nodes and elements cannot have any gaps or open spaces between them.
 - It cannot have any duplicated nodes.

- The surface element has to be orientable, which basically means that the orientation of the elements needs to be defined.

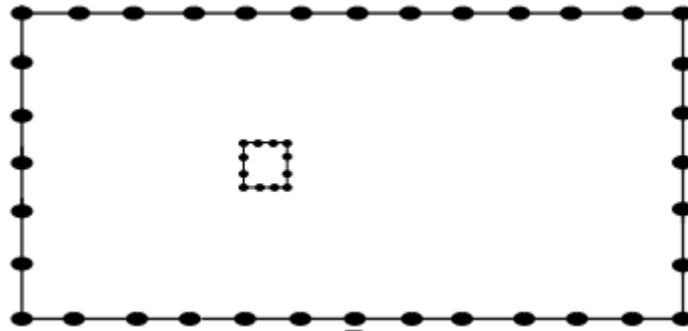


Figure 2.6. Defined nodes as black dots and element as lines [14].

- Then the solver uses the defined surface nodes and joins them together to create the triangle elements in the 2D case and tetrahedral element in the 3D case. This is the beginning for the mesh volume creation and at this step the Delaunay criteria is not fulfilled as shown in Figure 2.7 [14].

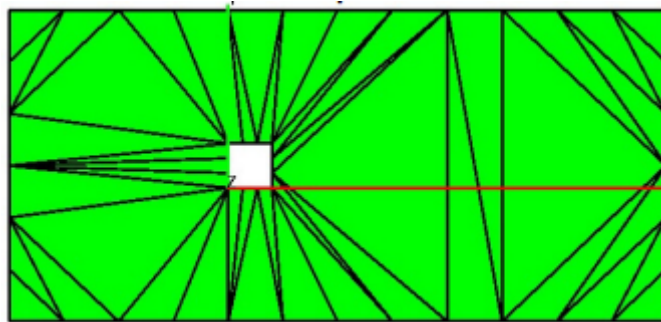


Figure 2.7. Connection of surface nodes that do not fulfill the Delaunay criteria [14].

- In the final step the solver adds nodes continually to the mesh, every time a node is added it will break down its main element into smaller elements that fulfill the Delaunay criteria, as shown in Figure 2.8. This process will be iterated based on linear interpolation until the set mesh criteria is fulfilled for example the desired mesh size [14].

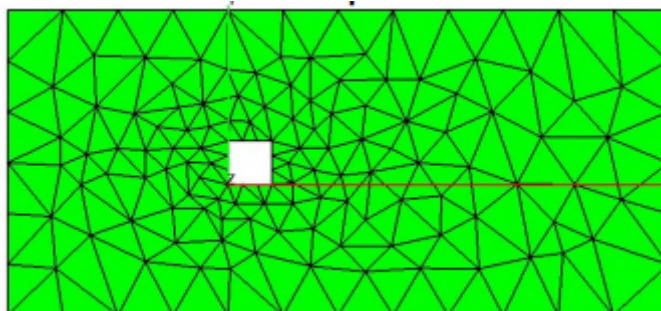


Figure 2.8. Final mesh structure that fulfills the Delaunay criteria [14].

Re-meshing

When FSI couplings are used, the solver will be using the ALE approach as pointed out earlier. Large deformations can occur in the fluid mesh due to the ALE approach. Large mesh deformations are not desirable due to the unreliable results. To avoid large deformations LS-DYNA have, by default, a re-meshing setting that only re-meshes inverted elements which are common in rotational problems. To improve re-meshing a ICFD_CONTROL_ADAPT_SIZE card can be used, which re-meshes the distorted elements with a frequency of the user's choice [14].

2.3.3. Lagrangian description

The Lagrangian mesh is a mesh structure with coinciding mesh points and material points. This means that no material passes through the elements and that the mesh deforms with the material as you can see in Figure 2.9. The Lagrangian mesh is best suited for solid mechanics simulations where the material is subjected to small deformations [15].



Figure 2.9. Lagrangian mesh showing how deformation of the body is deforming the mesh [15].

Advantages with the Lagrangian mesh

- It is easy to keep track of boundaries and interfaces because they coinciding with the mesh points.

Disadvantages with the Lagrangian mesh

- The mesh deforms with the body, which can lead to distortion with large deformations. Large distortions are unreliable and can lead to wrong results.

2.3.4. Eulerian description

The Eulerian mesh is a specially fixed mesh that do not deform with the material see Figure 2.10, where the body is the illustrated in gray deforms while the mesh stays the same. This type of mesh is good for chaotic bodies with a lot of movements and deformations which makes this mesh type preferably used for fluid mechanic simulations [15].

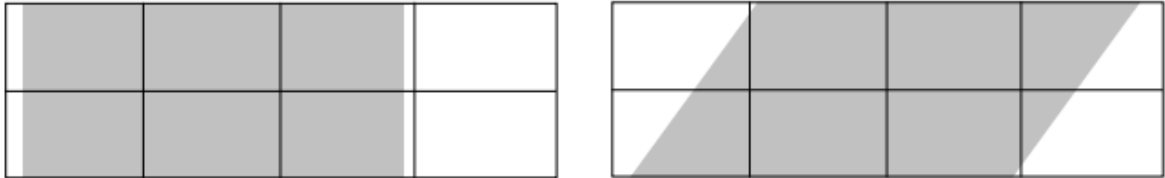


Figure 2.10. Eulerian mesh showing how deformation of the body does not deform the mesh [15].

Advantages with the Eulerian mesh

- The mesh stays fix and distortion does not occur.

Disadvantages with the Eulerian mesh

- It is difficult to keep track of boundaries and interfaces because they do not coincide with the mesh points.

2.3.5. Arbitrary Lagrangian-Eulerian Description (ALE)

When using pure CFD simulation then the Eulerian formulation is used on the fluid domain as mentioned earlier. The Eulerian mesh is not suited for FSI couplings due to the fact that it cannot keep track of the interface between the structure domain and the fluid domain.

To enable the Fluid domain to keep track of the interface a Lagrangian description is added to the Eulerian mesh at the interface, which changes the characteristics of the mesh and an Arbitrary Lagrangian-Eulerian description is obtained also known as ALE. In Figure 2.11 an illustration of the difference between ALE and Lagrangian description is shown where the Lagrangian mesh have larger mesh deformations which leads to unreliable results [14].

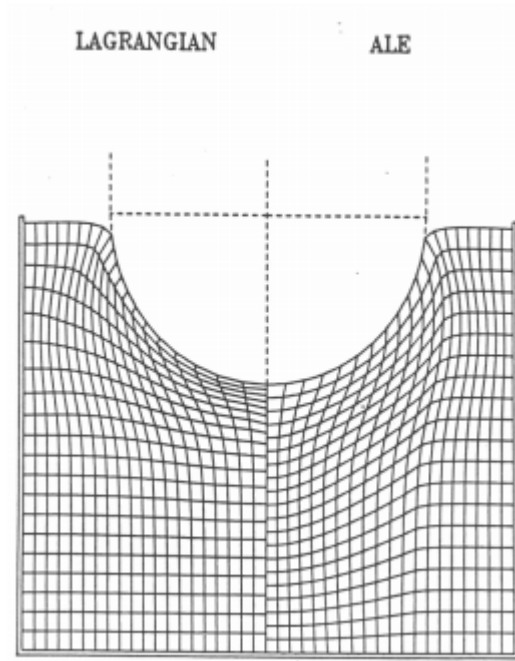


Figure 2.11. Difference between Lagrangian and ALE approach [15].

Advantages with the ALE mesh

- Likewise, for the Lagrangian description and interfaces is coinciding with the mesh points.
- The distortion is minimal

Disadvantages with the ALE mesh

- Likewise, for the Eulerian description the material points are passing through elements

2.3.6. Level set method

To the fact that ICFD simulations often have more than one type of material that interact with each other, for example water and air, oil and water or even oil and vacuum, a level set method is used. The level set method is a fast and reliable technique that keeps track of the moving interfaces to represent the fluid dynamics.

The level set method is using an implicit function ϕ which is defined for the whole fluid volume in 3D simulations and the whole fluid area in 2D simulations, while the interface is defined as one dimension lower, as a surface area in 3D and a line in 2D. The interface between two mediums are defined as $\phi = 0$, while the lower medium is defined as $\phi < 0$ and the upper medium as $\phi > 0$ [14]. ϕ will also be defined as a distance function which is resulting in the level set function,

$$\phi(\vec{x}) = \min(|\vec{x} - \vec{x}_l|) \quad \text{on } \Omega^+, \text{ for all } \vec{x}_l \in \partial\Omega, \quad (2.17)$$

$$\phi(\vec{x}) = 0 \quad \text{on } \partial\Omega, \text{ for all } \vec{x}_l \in \partial\Omega, \quad (2.18)$$

$$\phi(\vec{x}) = -\min(|\vec{x} - \vec{x}_l|) \quad \text{on } \partial\Omega^-, \text{ for all } \vec{x}_l \in \partial\Omega \quad (2.19)$$

Because ϕ is the Euclidean distance,

$$|\vec{\nabla}\phi| = 1. \quad (2.20)$$

All this is illustrated in Figure 2.12 for a simple dam problem [14].

Initial state of dam problem

Deformed state of dam problem

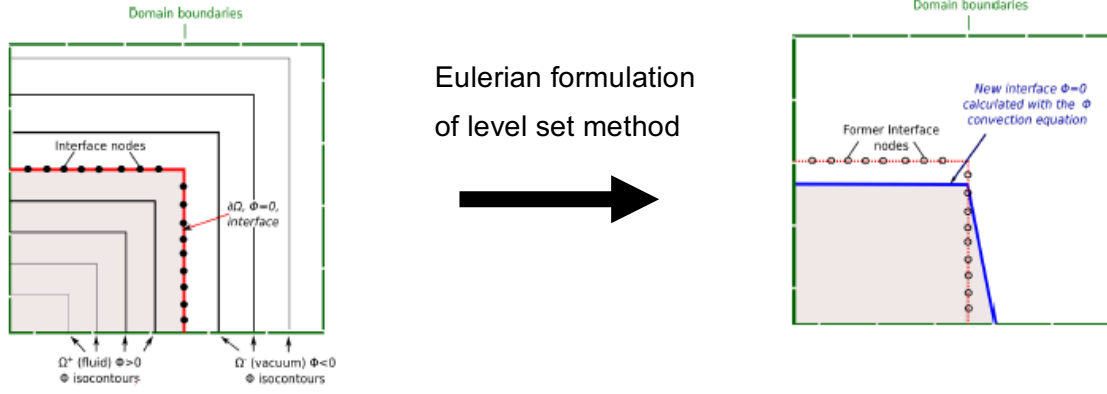


Figure 2.12. Illustrates the level set method in form of a simple dam problem [14].

A convection equation is used to define the implicit functions evolution [14],

$$\frac{\partial\phi}{\partial t} + \vec{V} \cdot \vec{\nabla}\phi = 0. \quad (2.21)$$

To find a weak form of equation (2.22) to enable integration over a defined domain, the Galerkin method is used which results in the following equation, for more information see [14],

$$\int_{\Omega} N_1(1.5\phi_i^{n+1} - 2\phi_i^n + 0.5\phi_i^{n-1})d\Omega + \int_{\Omega} \Delta t N_i u_j^n \frac{\partial\phi_i^{n+1}}{\partial x_j} \partial\Omega = 0. \quad (2.23)$$

Which gives the matrix form

$$\mathbf{M}(1.5\phi_i^{n+1} - 2\phi_i^n + 0.5\phi_i^{n-1}) + \Delta t \mathbf{S}(u_i^n)\phi_j^{n+1} = 0, \quad (2.24)$$

The final system is obtained after a stabilization process [14],

$$\mathbf{M}(1.5\phi_i^{n+1} - 2\phi_i^n + 0.5\phi_i^{n-1}) + \Delta t \mathbf{S}(u_i^n)\phi_j^{n+1} - \tau(\mathbf{S}_y(u_i^n)\psi_j^n - \mathbf{S}_u(u_i^n)\phi_j^{n+1}) = 0 \quad (2.25)$$

$$\mathbf{M}\psi_i^n - \mathbf{C}(u_i^n)\phi_j^n = 0 \quad (2.26)$$

2.4. Structure domain

There is many ways to define a solid body in LS-DYNA, but only the rigid body definition will be further explained. The rigid body is basically defining a structure without any deformations which means that for any two given point on the structure the distant is constant during the simulation process. Defining a structure as rigid is preferred when small or no forces are applied on the structure because then it becomes an approximation of the real case [14].

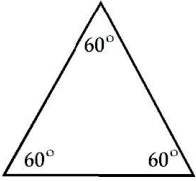
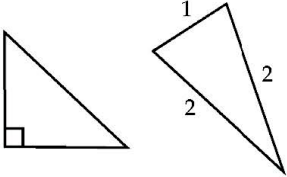
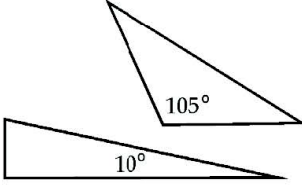
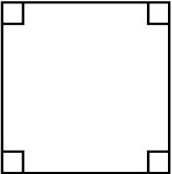
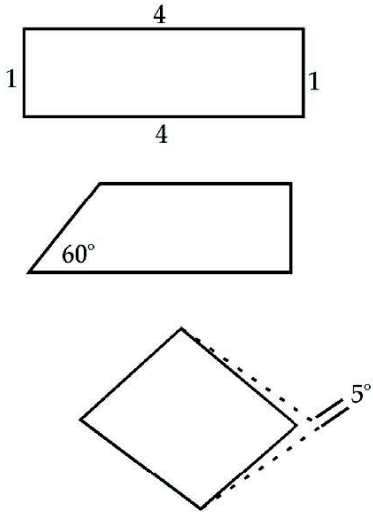
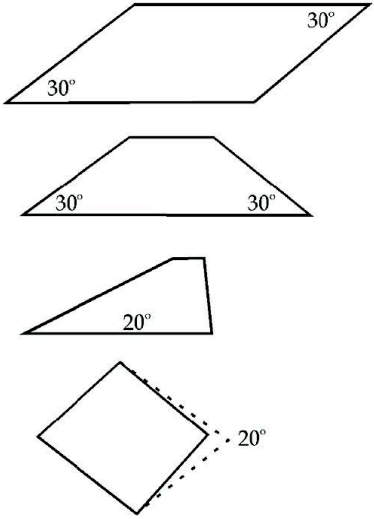
2.4.1. Mesh

The meshing process is performed manual on the structural domain and the meshing possibilities are endless where you can choose what type of element and element size to use, mix different element and element size types to obtain the correct description of your structure, manually reshape one element with bad geometry and so on [16].

When meshing manually with a huge variety of elements it is easy to acquire undesirable geometries of elements, see Table 2.1, which means elements with shapes that provides wrong results. The element geometry is limited by the structure geometry and sometimes undesirable elements are unavoidable and the user have to use experience and commonsense to solve the problem or relocate the bad element to a position where it does not affect the required result. If the mesh program has quality check, then it is preferable to always use it because a bad mesh can give wrong results and sometimes it is hard to identify elements with undesirable geometry when your system contains of thousands of elements [16].

The best geometry regarding a three node element is when the triangle is equilateral and all the angels are 60° and same goes for the fore node elements which forms a square with 90° angels. An acceptable angel regarding the three node element is approximately in the rage between 30° to 100° , while for the four node elements it is in the range between 60° to 120° . This can be seen in Table 2.1 where the element qualities and their definitions are illustrated [16].

Table 2.1. Illustrated element qualities.

Best	OK	Undesirable geometric shape
 <p>An equilateral triangle with all three interior angles labeled as 60°.</p>	 <p>A right-angled triangle with a right angle symbol at the bottom-left corner. Next to it is a scalene triangle with two sides labeled '1' and '2'.</p>	 <p>Two triangles. The top one has an obtuse angle of 105°. The bottom one has a very small acute angle of 10°.</p>
 <p>A square with right angle symbols at each of its four corners.</p>	 <p>Three rectangles: a square with side lengths labeled '1' and '4', a rectangle with a 60° angle, and a diamond shape with a 5° angle indicated by a dashed line.</p>	 <p>Four parallelograms with angles of 30°, 30°, and 20°. Below them is a diamond shape with a 20° angle indicated by a dashed line.</p>

3. Method

3.1. Design of Experimental Setup

In order to validate the numerical models an experimental setup of the wet clutch system had to be designed. To ensure a versatile experimental setup, where changes in parameters and measurements can be done, many aspects need to be considered such as which parameters that are dependent, what measurements that are required etc. The numerical models need to be simplified to decrease the calculation time of the simulations in LS-DYNA. The experimental setup has a simple geometry in order to decrease modelling errors. These simplifications will also make for more stable and easily controlled tests and will most likely decrease the amount of error sources, which also naturally occur in physical experimenting.

3.1.1. Conceptual Design Aspects

The conceptual design aspects in this section will act as a guide to reach a final design of the experimental setup. Aspects concerning the clutch drum, clutch housing, measurements and the external fixture will be set.

Clutch drum

As the numerical models are intended to calculate the drag losses as well as mimic the oil flow behavior around the clutch drum of a wet clutch, including the simplifications, the components for the wet clutch test setup can be decreased and simplified as well. As seen in Figure 3.1 a wet clutch drum consists of many components (left), many that can be simplified or simply removed (right).

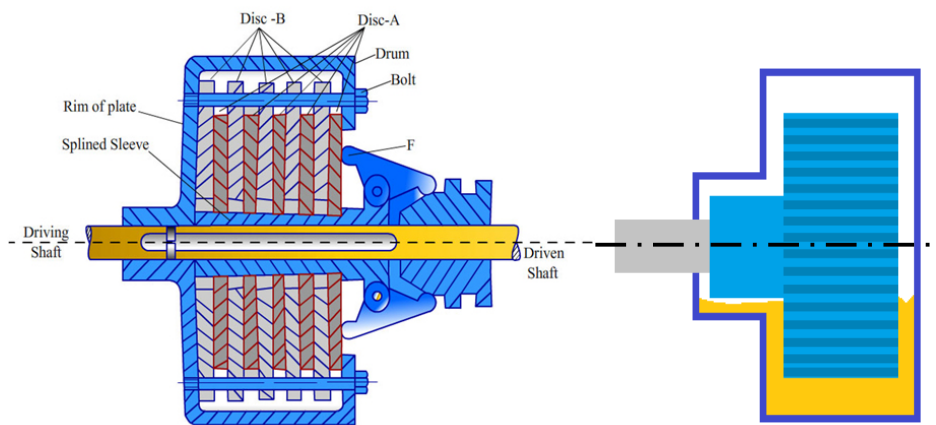


Figure 3.1. Clutch drum components (left) [17], simplified clutch drum (right).

The first step towards simplifying the test setup is therefore to remove the friction and separator discs and fully enclose the clutch drum. This will result in elimination of the losses tied to shearing of the oil inside the clutch drum. The outgoing shaft of the clutch drum will also be removed as the test setup will not transfer any torque in between shafts.

Clutch Housing

The design of the wet clutch housing setup was based on the test setup used in previous projects as mentioned earlier in this report. As the numerical model also will include an oil sump, where the clutch drum shoots oil out from the cylinder to cool down, it has to be included in the test setup as well. This can be seen in Figure 3.2 below.

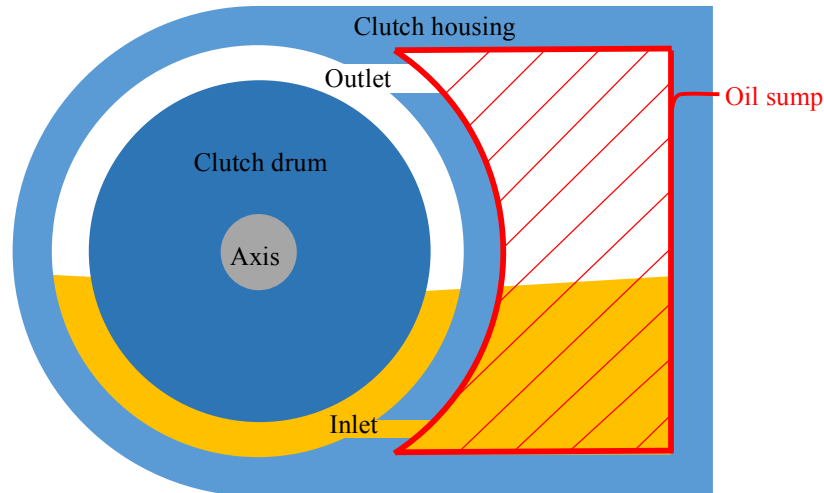


Figure 3.2. Cross section of wet clutch housing concept.

The oil travels back and forth between the cylinder and oil sump through an inlet and outlet. The outlet is located in the upper right section of the cylinder (first quadrant) and inlet to the bottom right section of the cylinder (fourth quadrant). Thus it makes it possible for the clutch drum to drag oil from the bottom of the cylinder and throw it into the oil sump through the outlet in a horizontal tangential projection. This setup differs from a standard wet clutch setup as the oil often enters the cylinder through the clutch drum axially in order to spread between the lamellae for heat absorption and lubrication. The oil is then pushed out of the lamellae radially and enters the cylinder.

In order to make the test setup more versatile the housing is split up into four parts; the main housing, inlet, outlet and lid. This makes it possible to change the geometry and position of the inlet and outlet independent of each other resulting in an experimental optimization of the positioning of the outlet. The components in the wet clutch housing are illustrated in Figure 3.3, excluding the lid.

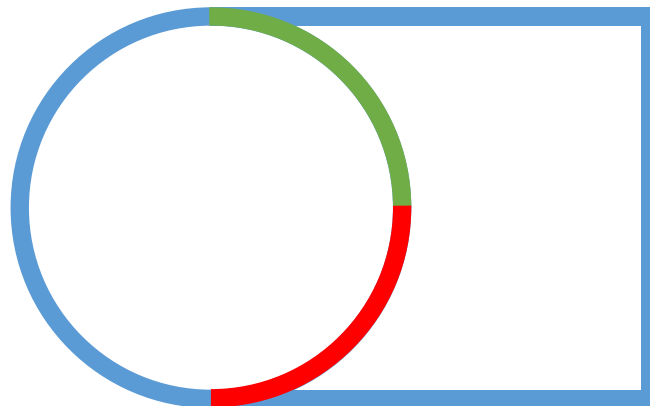


Figure 3.3. Components in wet clutch housing setup, housing (blue), inlet (red) and outlet (green).

Measurements & Sensors

The wet clutch housing setup is not complete without a way to measure and collect data for validation of the numeric models. Sensors need to be mounted on the housing, as this setup is intended to measure drag losses and oil flow behavior inside the wet clutch housing. The oil flow behavior will, like earlier projects in this field, be measured with a high speed camera. This method makes it easy to measure and collect data on the oil flow behavior. In order for the high speed camera to capture the flow behavior inside of the housing the exterior has to be transparent on all sides. This is due to the fact that high speed cameras need a lot of lighting in order to capture a higher amount of frames per second as the amount of light received by the shutter decreases as the shutter speed increases. The overall transparency will also enable measurements from different angles.

The rotating clutch drum inflicts a dragging force, acting on the housing, by churning of the oil. This can be measured with a dynamometer attached to the housing, which measures the acting force in the spot where the dynamometer is attached. The force is then used to calculate the drag torque inflicted on the housing and by measuring the torque with and without oil inside the housing it is possible to calculate the resulting torque implied by the drag force.

External Fixture

In order to measure the drag torque on the clutch housing the housing needs to be completely disconnected from the clutch drum's axis in order to remove the drag torque caused by the electrical motor and to be able to rotate independently from the clutch drum. The clutch drum instead hangs freely inside the housing and is supported by bearings connected to the external fixture outside the housing. The housing is attached to the external fixture with two bearings, which holds and separates the housing from the axis. This setup is illustrated in Figure 3.4 below, where the external fixture is presented in red.

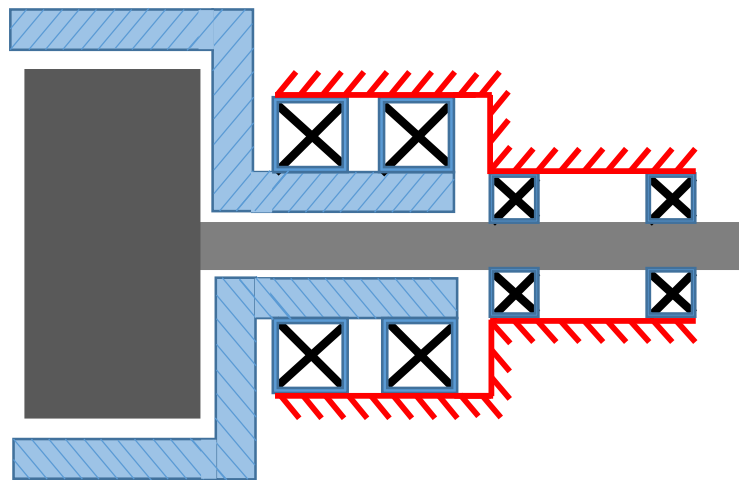


Figure 3.4. Bearing setup between clutch housing and axis

The electric motor will also be connected to the external fixture, which makes the test rig more portable as everything is connected to the external fixture.

3.1.2. CAD-model of Conceptual Design Aspects

The conceptual design aspects lead to a final design of the test setup, which includes the wet clutch housing, clutch drum and an external fixture, which holds every component together. The complete test setup, excluding the electric motor, can be seen in Figure 3.5 below.

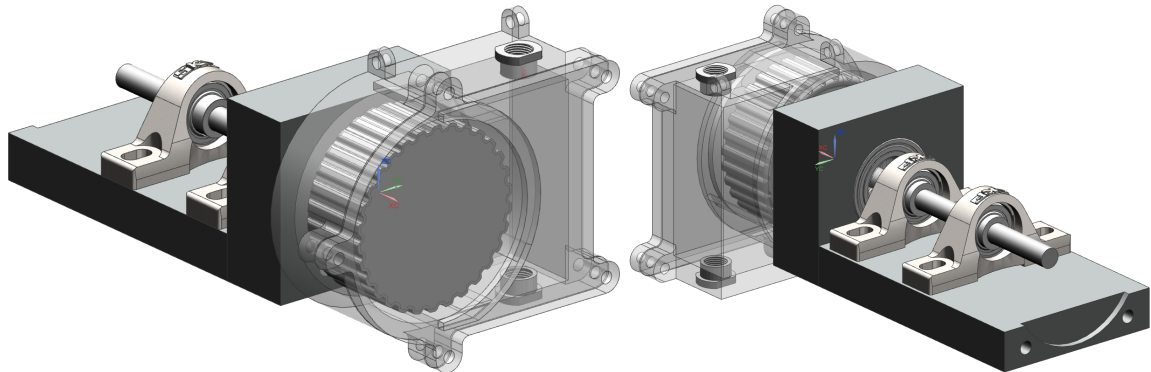


Figure 3.5. Complete test setup

In order to fully describe the components in the test setup the setup will be divided and explained individually as clutch drum, external fixture and wet clutch housing.

Clutch Drum

The clutch drum design is based on the clutch drum used in the Haldex LSC GenV. In order to minimize the simulation time of the numerical model, complex geometries need to be modified. As the numerical model does not compute shearing losses, which occur inside the clutch drum, the drum can simply be fully enclosed making it impossible for oil to get inside. A comparison of the original and modified drum can be seen in Figure 3.6 below.

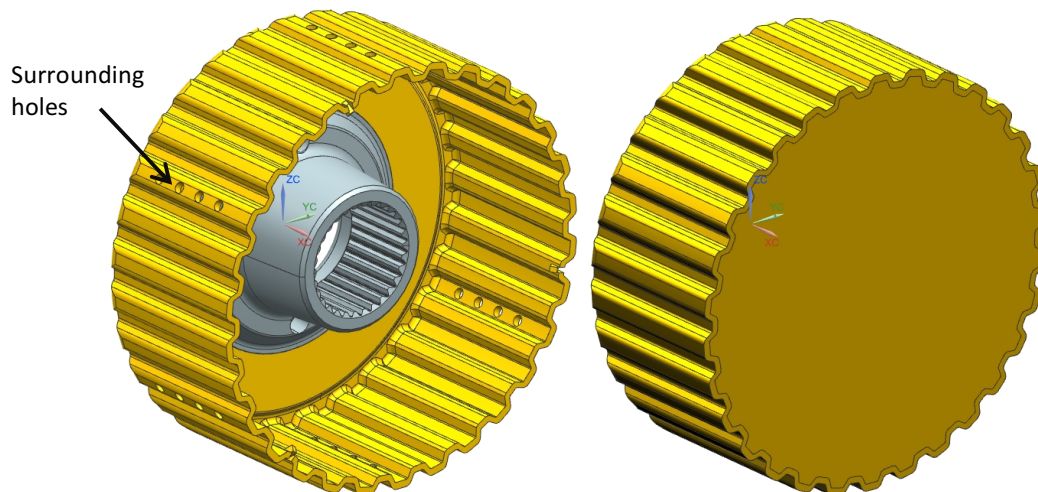


Figure 3.6. Original Haldex LSC GenV (left), modified clutch drum (right).

As seen in Figure 3.6 the end of the drum has been fully enclosed together with the holes surrounding the drum, which acts as an escape route for the used lubricant in between the friction and separator discs. Further

modifications had to be made to avoid unnecessary complexity to the clutch housing and axis mounting. These modifications can be seen in Figure 3.7 below.

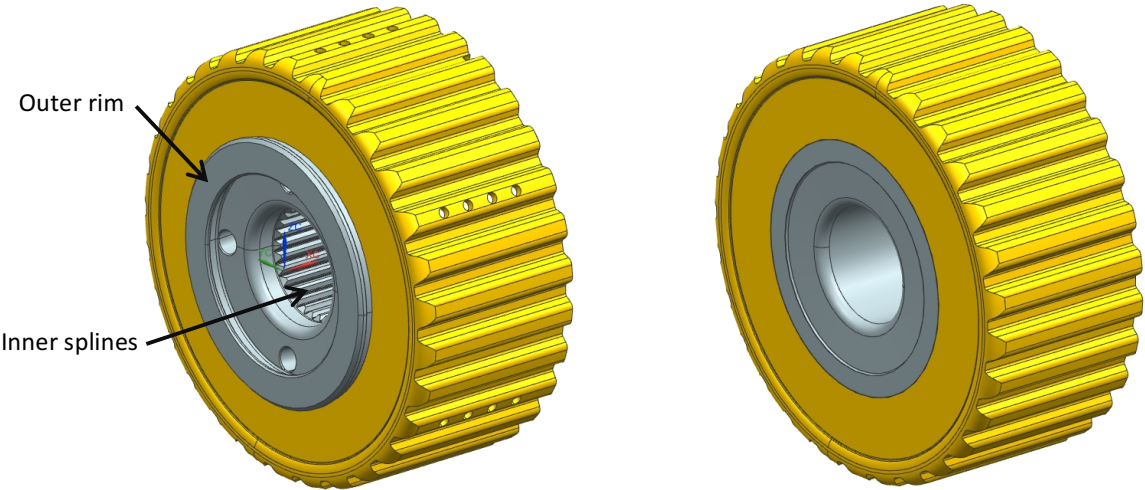


Figure 3.7. Original Haldex LSC GenV (left), modified clutch drum (right).

As seen in Figure 3.7 the outer rim of the inner fixture of the original clutch drum has been removed together with the inner splines. The holes on the inner fixture are also removed to fully enclose the clutch drum. The splines were removed to simplify the mounting on a shaft. As the applied torque and drag torque acting on the clutch drum are small the splines are unnecessary and would simply make it more difficult for mounting. The outer rim was removed as leaving it would require a groove in the clutch housing wall, which would increase complexity to the housing.

External Fixture and Choice of Bearings

As the external fixture only needs to hold everything together the design aspects does not affect the final design to the same extent as the other components. Instead the aspects for the external fixture come down to placement of bearings and electric motor, robustness and total weight of the test setup. To make the fixture easier to manufacture it is split into two components, a base plate and a bearing housing. The separate components can be seen in Figure 3.8 below.

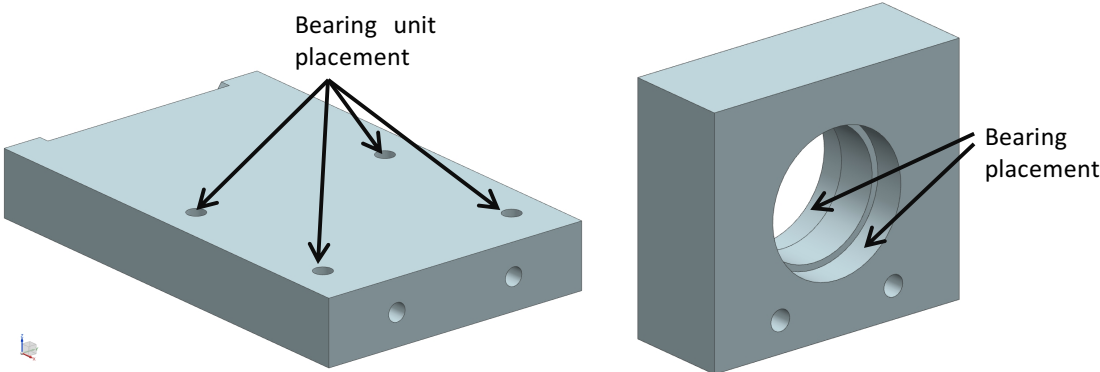


Figure 3.8. Base plate (left), bearing housing (right).

The bearing housing seen in Figure 3.8 was designed using the geometries of the chosen bearings for the mounting of the wet clutch housing. To make sure stability and load distribution of the mounting two bearings of the SKF 6008-2Z type was used, more information about the bearings can be found in Appendix A. The bearings will be press-fitted from each side of the bearing housing. Furthermore, the shaft between the electric motor and clutch drum will be held up by two bearing units, namely the SKF SY 15 TF. More information about these bearing units can be found in Appendix B. The bearing units will be mounted on the base plate seen in Figure 3.8 and therefore sets the positioning of the mounting holes. The mounting for the electric motor can be seen in Figure 3.9 below.

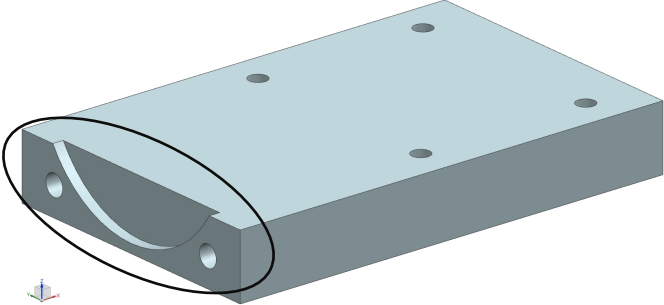


Figure 3.9. Mounting for electric motor

The groove on the end of the base plate is due to a flange on the electric motor. The flange aligns the electric motor to the shaft, which makes the dimensions of the groove important. All holes in the base plate are threaded in order to mount the components together. The assembled external fixture including bearings and bearing units can be seen in Figure 3.10 below.

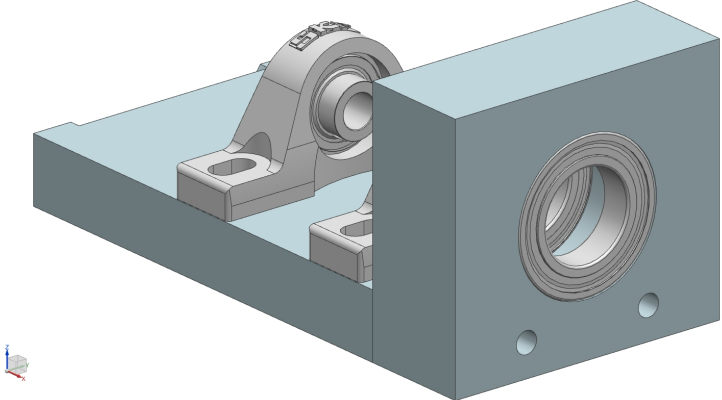


Figure 3.10. External fixture, including SKF 6008-2Z bearings and SKF SY 15 TF bearing units.

Wet Clutch Housing

The wet clutch housing contains many different components fulfilling different needs of the test setup. All components for the wet clutch housing was manufactured using Accura® ClearVue material, see Appendix C for more information. In order to make the test setup more versatile the inlet and outlet inside the housing are designed as different components making it possible to change them in size independent of each other. For a better understanding of this an exploded view of the wet clutch housing can be seen in Figure 3.11 below.

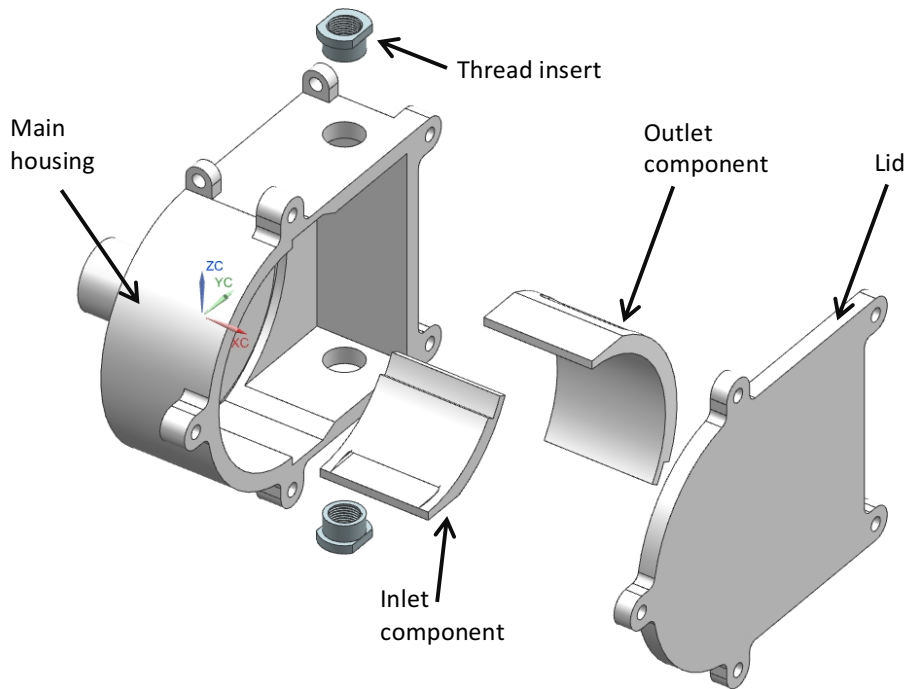


Figure 3.11. Exploded view of wet clutch housing.

The inlet and outlet components fit together with an overlap preventing any oil from leaking into the oil sump. The inlet and outlet components are then slotted into a groove in the housing constructing a wall between the housing cylinder, in which the clutch drum will rotate, and the oil sump. On the other side of the inlet and outlet components a lid containing the same groove as the housing. As the lid encloses the housing and locks in the inlet and outlet components it forms a cylinder chamber and an oil sump chamber, which are connected through the inlet and outlet. Both the inlet and outlet are designed in different sizes and the outlet is also designed in different angles of attack, meaning that the output can be placed later in the oil's rotational direction. For better understanding of this both the outlet and inlet are shown in section view in Figure 3.12.

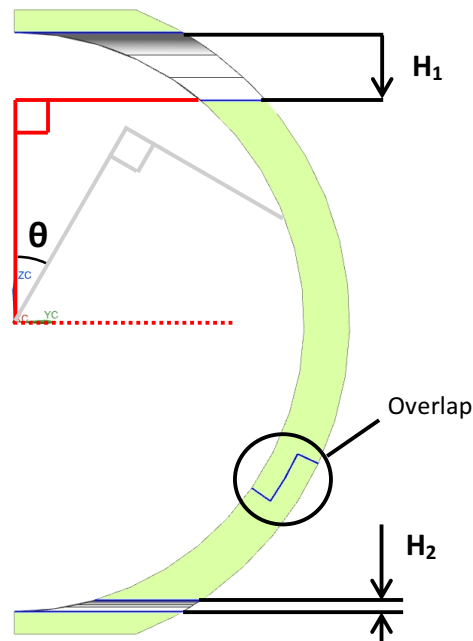


Figure 3.12. Section view of inlet and outlet.

In the section view of the inlet and outlet the joint is illustrated as well as the dimensions that will vary among the different inlets and outlets. Table 3.1 shows the different dimensions designed for the inlet and outlet components.

Table 3.1. Dimensions used to create different inlet and outlet components

Inlet component	Outlet component	
H_2 [mm]	H_1 [mm]	Θ [°]
2,5	15,0	0
5,0		15
7,5		30
10,0	10,0	0
	20,0	

This dimension setup results in four different inlet components and five different outlet components, where inlet and outlet can be changed independent of each other. The number of unique test setups will thereby be $4 \cdot 5 = 20$ ranging from different angles of incidence to different sizes of inlet and outlet orifice. A comparison between the 0 degree outlet and 30 degree outlet can be seen in Appendix D.

The thread inserts are designed to make it possible to connect an outgoing tube between the thread inserts. This tube makes it possible to measure the immersion depth of the oil inside the housing and also makes it possible to drain and refill the housing. The threaded inserts are threaded with a pipe thread size of 3/8" making it possible to connect both pipe nipples and pipe plugs of the same thread size.

The main housing of the test setup was designed with simplicity as a key design aspect. As the numerical models need to be as simple as possible in order to reduce simulation time it was important to only use simple geometries inside the housing. Therefore, the added oil sump is designed using simple straight edges aside from the other side of the cylinder wall. The main housing is illustrated in Figure 3.13 below, where a zoomed view of the shaft entrance also can be seen.

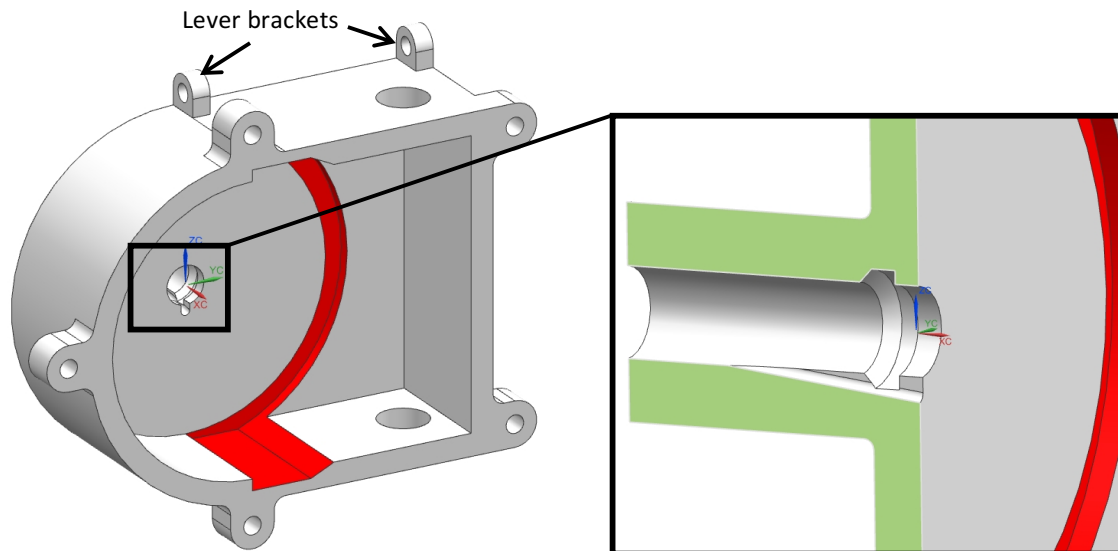


Figure 3.13. Main housing (left), zoomed section view of shaft entrance (right).

The red faces in Figure 3.13 illustrate the groove in which the inlet and outlet components are to be mounted. The shaft lies freely inside the shaft entrance to ensure no additional friction losses will occur and is not in contact with the housing at any time. This design had to be made to ensure measurement of such small drag torque losses the rotating clutch drum implies. However, it leaves a gap in between the shaft and the housing where oil can escape. The design of the shaft entrance, which can be seen in the zoomed section view of Figure 3.13, forces the oil back into the housing through a conduit. A radial track stops the oil from wandering further into the shaft entrance by the use of centrifugal forces that hurls the oil in a tangential projectile into the track, which then flows down to the conduit and back into the housing.

The lever brackets are designed to be able to mount a lever which can be used to balance the house horizontally as the house can rotate freely on the external fixture. The lever will also be used to be able to fasten and position the dynamometer or load cell used to measure the drag torque.

In order to mount the housing onto the external fixture an extended shaft from the housing was designed, which can be seen in Figure 3.14 below. The shaft will be mounted on the two bearings seen in Figure 3.10.

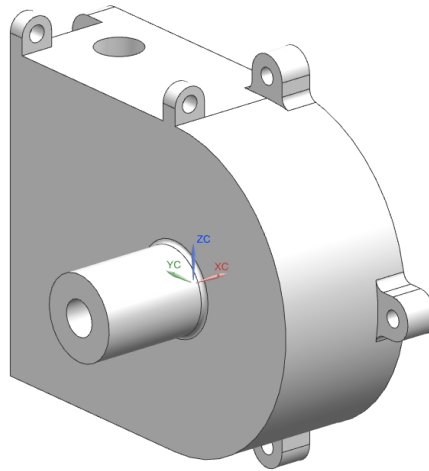


Figure 3.14. Illustration of mounting shaft on the main housing.

Extension of Wet Clutch Housing

The 2D numerical model does not take edge-effects into account since the problem only can be defined in one plane. This numerical model does not take into account the fact that there is a gap between the clutch drum and clutch housing other than the obvious gap between the housing cylinder and clutch drum. To limit the influence of the edges on the clutch drum a simple extension can be made to the clutch housing to proportionally decrease the influence of the edges. An exploded view of the extended clutch house can be seen in Figure 3.15 below where new inlet and outlet components are designed as well.

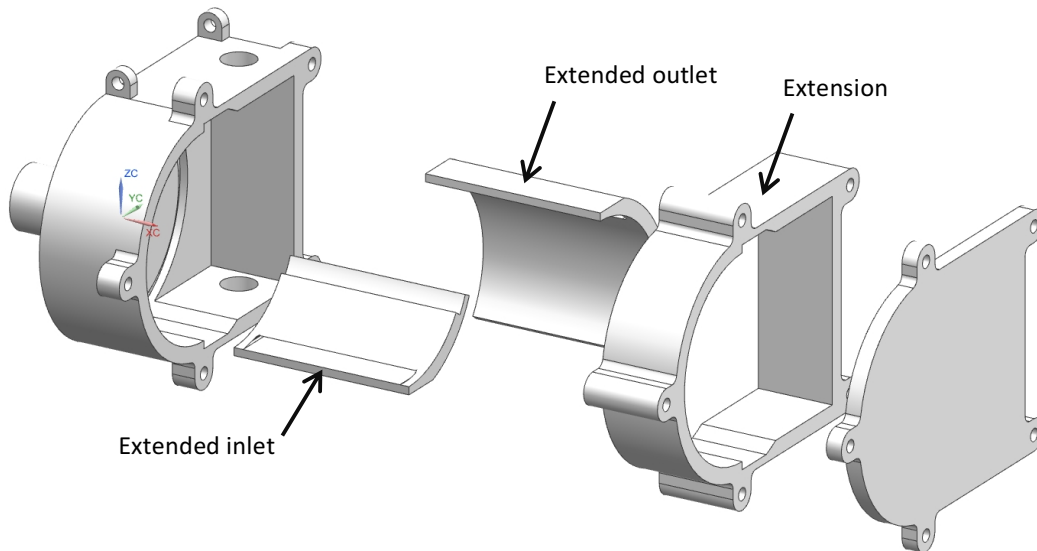


Figure 3.15. Exploded view of extended wet clutch housing.

The extended inlet and outlet components are designed using the dimension setup listed in Table 3.1. The extension of the wet clutch housing will make the gaps between the clutch drum and housing proportionally

smaller compared to the length of the housing and better experimental data can be collected to validate the 2D numerical model. The assembled housing can be seen in Figure 3.16 below.

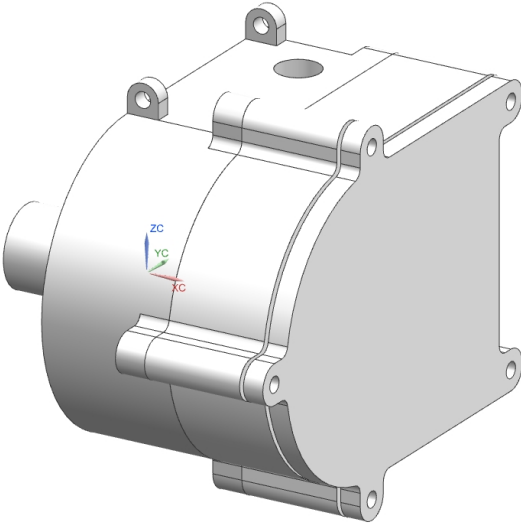


Figure 3.16. Assembled view of the extended wet clutch housing.

The clutch drum in this extended setup is simply two clutch drums put together, as illustrated in Figure 3.17 below.

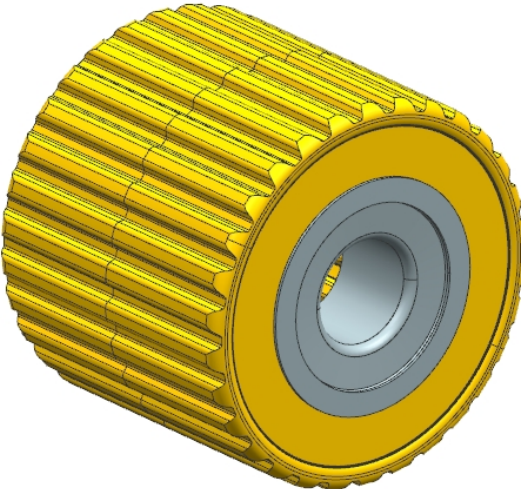


Figure 3.17. Illustration of extended clutch drum.

3.1.3. Volume Verification of Wet Clutch Housing

A volume verification was done in order to make sure that oil sump volume would not be too small and prevent the oil flow in any way. This was done by setting the desired immersion depth of the clutch drum and then calculating the volume surrounding the clutch drum using Siemens NX and adding it to the volume of the oil sump. If the oil sump would be completely filled the immersion depth needed to be decreased. As the shaft between the electric motor and clutch drum lies freely in the shaft entrance of the house and leaves a gap, the oil immersion depth is constrained at all time to be below the gap.

3.1.4. Structural Analysis of Test Setup

A structural analysis was conducted on the shaft and the wet clutch housing, using Siemens NX, in order to predict the displacements and stresses. This was done to assure that the clutch drum cannot at any time be in contact with the housing as it would destroy the transparent surface of the housing as well as the desired results of the experiments.

Shaft

The shaft was modeled using standard steel which could be found in Siemens NX material database. Cylindrical constraints were applied to the surface area in which the bearing units held the shaft. A load was applied and over dimensioned with a safety factor of 2.5 at the very end of the shaft to make sure the shaft's structure strength meets the requirements. The model setup of the structural analysis can be seen in Figure 3.18 below where the cylindrical constraint and load is illustrated.

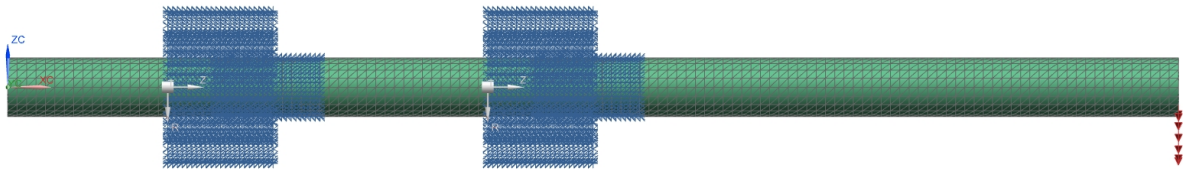


Figure 3.18. Structural analysis model setup of the shaft.

The resulting displacement and stresses lies within the requirements and the displacement does not affect the tilt of the clutch drum in a way that it would collide with the wet clutch housing. The results and material data of the structural analysis can be found in Appendix E.1.

Housing

The structural analysis of the housing was done similarly to the analysis of the shaft. Cylindrical constraints were set on the surface area on which the bearings are mounted. A load pointing downward was applied and over dimensioned with a safety factor of 2.5 at the very end of the housing. The material was set to acrylic which could be found in Siemens NX material database. The material data and results from the structural analysis of the wet clutch housing can be found in Appendix E.2.

3.2. Numerical Model

As the final design of the test setup was set the creation of the numerical models started. The numerical models consist of a 2D and 3D model of the wet clutch housing and drum created using Siemens NX, LS-PrePost and LS-DYNA. Setting up a problem simply using LS-PrePost together with the LS-DYNA solver can be done easily when it comes to simpler geometries as the tools for meshing does not require any solid surfaces or sheet surfaces. Although it can be done solely using Dynamore's software it becomes problematic when it comes to the geometries of the wet clutch. Instead Siemens NX was used to mesh all the geometries in the wet clutch and as the test setup was designed using Siemens NC it was natural to continue the meshing in Siemens NX using the finite element method. The mesh was then exported to LS-DYNA formatting and imported to LS-PrePost where the setup of the model was done. The model was then sent to the LS-DYNA solver to be calculated generating a post-processing file. The post-processing file was then opened in LS-PrePost for analyzing.

3.2.1. Model structure

The structure of the numerical model lays the foundation of how it might be used in the future and it is therefore important to make versatile so that the model can be applied to many different wet clutch systems. The numerical model is therefore split up where the mesh and model are separated. Also when it comes to a model including FSI the structure and fluid will be separated having its own model where a model that does not include FSI simply does not have a structure problem to solve. A mapping of the FSI integrated numerical model can be seen in Figure 3.19 below.

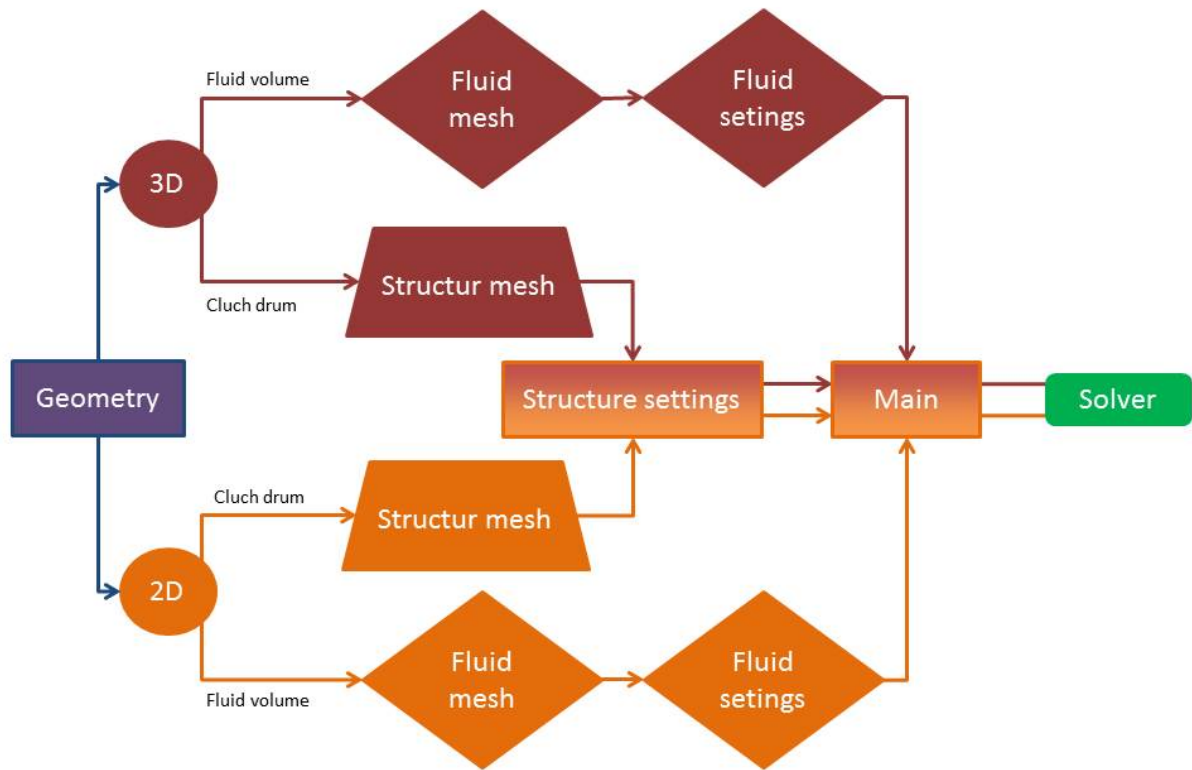


Figure 3.19. Mapping of numerical model with FSI problem.

As seen in Figure 3.20 below, the numerical model with no FSI problem is much simpler and will thereby be faster to simulate.

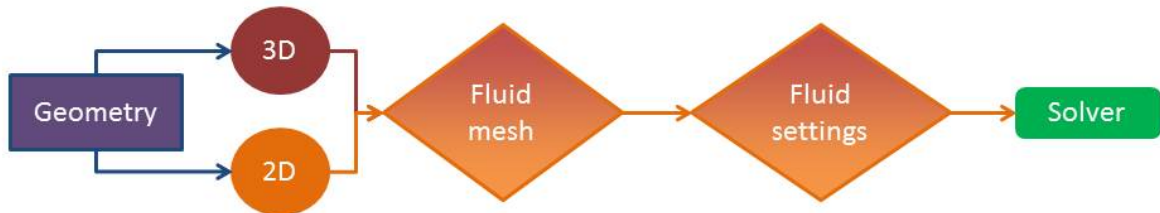


Figure 3.20. Mapping of numerical model without FSI problem.

3.2.2. Geometry & Meshing

As mentioned above the preparation of the numerical model started using Siemens NX. As the ICFD solver in LS-DYNA works by combining ICFD parts and generating the volume mesh it is necessary to have this in mind when creating the mesh in Siemens NX. First and foremost, the CAD model of the wet clutch housing needed to be prepared. As the numerical models will not include a structural analysis of the actual housing and only focuses on fluid analysis the only important geometries of the housing are the inner walls. Only using the inner walls will instead generate a fluid volume which can be seen in Figure 3.21 below.

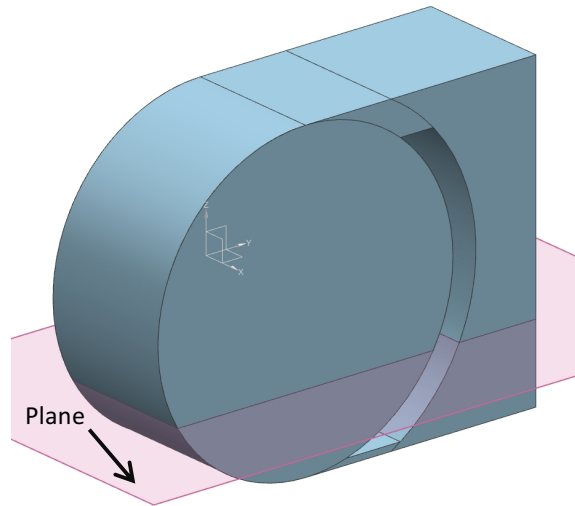


Figure 3.21. Fluid volume of wet clutch housing.

The fluid volume is also split in two by a plane shown in Figure 3.21 to separate the different fluid mediums used in the numerical model. Further modifications to the fluid volume needs to be done to include the clutch drum. By simply subtracting the clutch drum volume from the fluid volume the clutch drum will be represented as well inside the fluid volume, which can be seen in a section view in Figure 3.22 below.

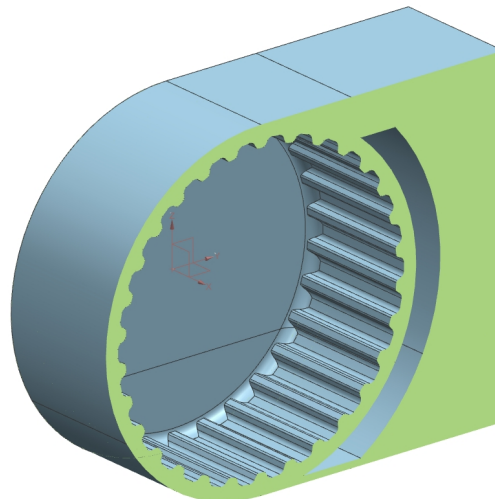


Figure 3.22. Section view of fluid volume including the clutch drum.

As the preparations of the geometries are done, the schematics of how to setup the ICFD parts needs to be set. The fluid volume must be divided into sections in order for the ICFD solver to generate the correct part volumes. A part volume is a representation of a medium's volume and as the numerical model will contain two different mediums, oil and void, two different part volumes needs to be defined. The ICFD part schematics applied to the fluid volume can be seen in Figure 3.23 below.

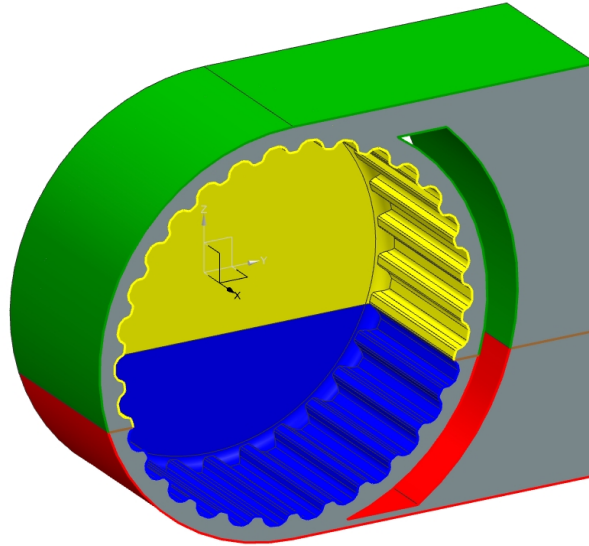


Figure 3.23. ICFD part schematics of fluid volume.

In the ICFD part schematics the different parts to be defined are illustrated using different colors. The reason for this many parts are due to the different mediums inside the wet clutch housing. The interface between the oil and void divides both the inner walls of the clutch housing and the clutch drum generating two parts for the housing and two parts for the drum. In between the two parts of both the housing and drum lays an interface that depending on the dimension of the numerical model will have one interface part for 3D or three interface parts for 2D. The reason for this is that in the 3D model the mediums can flow freely around the clutch drum, thereby the interface also surrounds the drum, where as in the 2D representation of the model the mediums can only flow around the drum and not in front and behind. A simplified ICFD part schematic for the model can be seen in Figure 3.24.

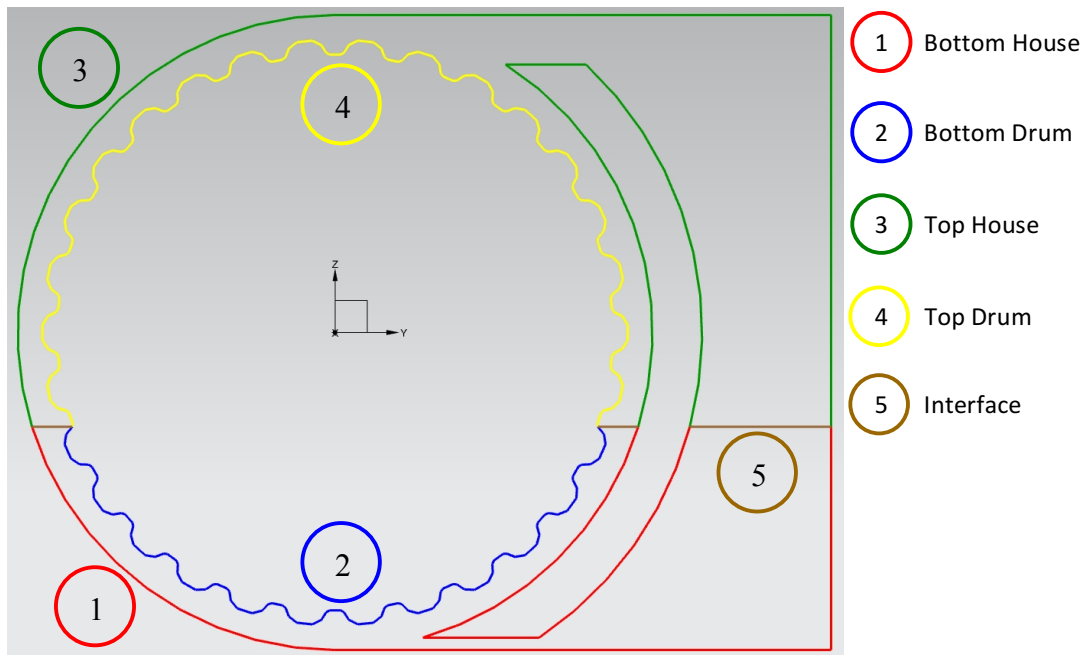


Figure 3.24. Simplified ICFD part schematic for 3D model.

The geometries were meshed with an element size of 0.5 mm, 1.0 mm and 2.0 mm in order to perform a mesh study. The simulations will have the exact same parameters except for the mesh size. The mesh study will determine what element size that will be more suitable for predicting drag torque and what element size that will be more suitable for fluid flow characteristics.

The ICFD solver in LS-DYNA generates a volume mesh from either shell elements or beam elements. If the numerical model is based on a 3D model the geometries need to be meshed using 4N shell elements, meaning that each element consists of four nodes at each corner. On the other hand, if the numerical model is based on a 2D model the geometries need to be meshed using 2N beam elements, meaning that each element consists of two nodes at each end of the element. In a 2D model the ICFD solver generates volume mesh that basically is a mesh of the area surrounded by the beam elements. It is also important that the element size is consistent throughout the whole model when it comes to the beam or shell elements.

3.2.3. Model Setup

The numerical model was set up using LS-Pre-Post, where different cards are used to create the model. Each card defines something in the model e.g. material data, loads, constraints etc. and together forms the complete model. A mesh file for example contains one card for all the elements and one card for all the nodes. The mesh file can then be included in the main file by a card that defines included files. This way it is very easy to edit the numerical model as everything is organized. The 3D numerical model consists of five files namely structural mesh, fluid mesh, structural main, fluid main and a main file connecting everything. The files can be opened using any text editing software and be easily edited. The advantage of separating the model into a fluid model and a structure model is that they can be run separately, to facilitate bug fixing.

3.2.4. Simulation

The simulation process took place in a cluster where it was possible to use multiple nodes for solving the numerical model. Each simulation ran on 32 nodes to reduce the simulation time and the cluster allowed for different simulations running at the same time. All the simulations were based on the same base model where changes in the parameters such as rotational speed, oil viscosity and house geometry generated different simulations. The parameters used in the simulations were set by the experiments on the experimental setup, to ensure that the collected data from the experiment was good and could be analyzed. When the parameters were set they were updated to the base model making a new numerical model that could be simulated. The numerical model was the run by the LS-DYNA solver and then analyzed when the simulation had stopped.

3.3. Experiments

The experiments where conducted in the wet clutch housing that was designed and explained in previous section. All the simplification that were made on the drum for the numerical model where also made for the experimental setup to make the setup as similar to the numerical model as possible. To fill the holes in the clutch drum provided from BorgWarner epoxy where used.

The main objective with the experiments was to capture the oil characteristics in form of oil flow and measure the drag losses generated from the oil depending on different geometries within clutch housing and different rotational speeds on the clutch drum.

3.3.1. Experimental Setup

The experimental setup consists of the test setup mentioned in previous section and shown in Figure 3.5, electrical motor with associated frequency converter, laptop, thermometer, oil, load cell and high-speed camera with associated high power lamps. The equipment used can be seen in Figure 3.25.

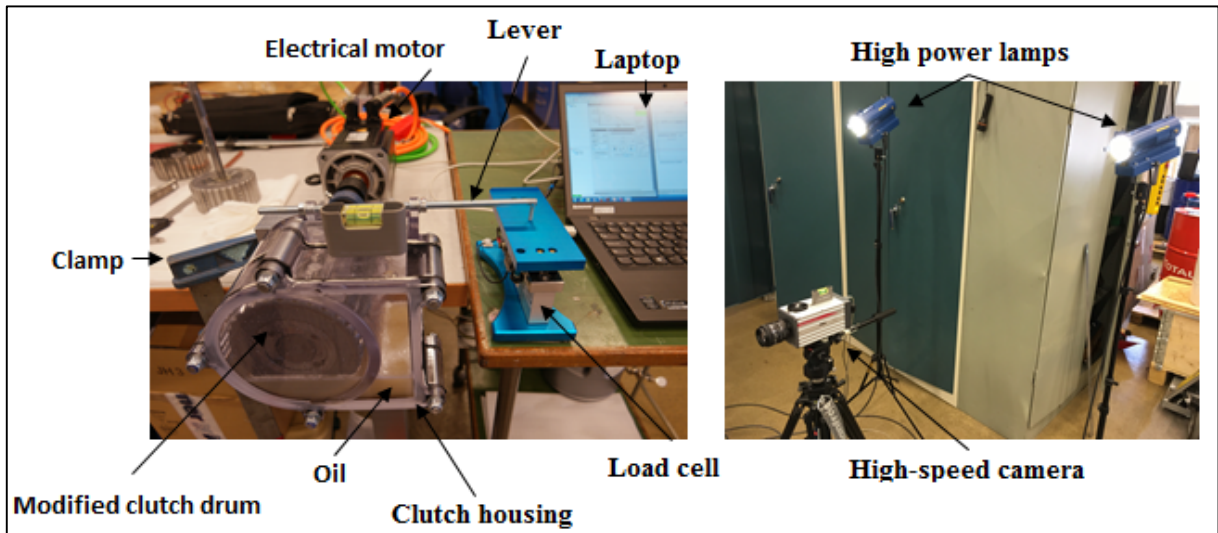


Figure 3.25. The experimental tools.

Early in the experiments, it was realized that on speeds over 500 rpm too much vibrations interfered with the sampling of data. The vibration problem was partly solved by clamping the test setup to a steady table while having a 2mm rubber gasket in between, which made the vibration interfere at speeds over 1000rpm.

The motor and frequency converter is from SEW-Eurodrive. The motor has a maximum rotational speed of 3000 rpm and the frequency converter is used to get as accurate and constant rotational speed as possible. The load cell is a ForceBoard, which measures the force mechanically in Newton and has an accuracy of 0.001 N. Measuring the losses mechanically is far more accurate and reliable than measuring energy consumption on the electric motor. As the energy losses in this system is very small the benefits are clear in using mechanical measurements. In order to increase the measured force on the load cell a lubricant with a higher viscosity than what is found in normal wet clutch systems was used. The oil that was used is called Gearway S5 75w-140 from Statoil. It has a kinematic viscosity of 140 cSt at 40 degrees Celsius and was assumed having the same temperature as the room which was measured with an electrical thermometer.

The high-speed camera was positioned on two different positions, one directly in front of the housing so that it is aligned with the center of the clutch drum as in Figure 3.26. The second position was from the left side of the housing where the camera is raised and filming from above with a 45-degree angle as in Figure 3.27. The camera is also supported with two 150W lamps to brighten up the recording area.

Top View

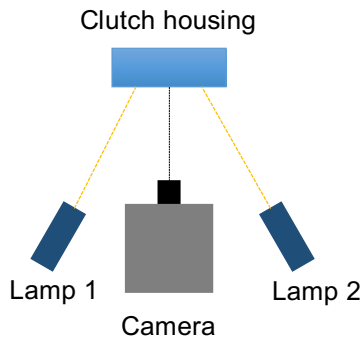


Figure 3.26. The first camera position.

Front View

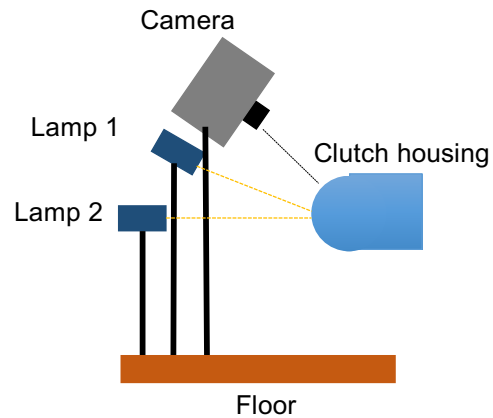


Figure 3.27. The second camera position.

3.3.2. Experimental Procedure

First of all, the geometry of the housing was decided where three different geometries were tested. The different geometries and their values can be seen in Table 3.2. The experimental procedure was reset between the geometry changes.

Table 3.2. Different geometries of the clutch housing.

Geometry	Inlet [mm]	Outlet [mm]	Angle [°]
1	2.5	15	0
2	10	15	0
3	10	15	30

The experimental procedure starts with reading the temperature, which was 22 degrees Celsius and was used to calculating the viscosity of the oil. Oil viscosity at 22 degrees Celsius is 480 cSt. The oil was then added to the housing and the oil surface was set to 45 mm from the bottom.

Four different rotational speed were decided to be investigated, see Table 3.3. The lowest speed were set by investigating the maximal rotational speed that was possible to obtain without having any oil leaving through the outlet, which is 250rpm regarding Geometry 1. The motor were set to a ramp up time of 0.06 seconds to the desired rotational speed.

Table 3.3. Investigated rotational speeds.

Rotational speed [rpm]
250
500
1000
1500

Two different laptops were used, one to regulate the rotational speed of the motor with the program Movitools and to sample the data from the load cell. The load cell was set to a sample frequency of 40 Hz, all sampling was repeated 10 times and an average of the tests was calculated to smoothen out the data and get better data to analyze.

The second laptop was used for the high-speed camera that was set to record in 1000 frames per second and recorded for 3 seconds after start.

3.3.3. Preparation of data

The sampling from the load cell and start of motor were manually started and stopped which led to different data intervals, which meant that all the data had to be manually prepared. This was done in Matlab, where a script was made that identified a common point for all data files, which was used to align all the sampled points and then the sampling time was set to the shortest sampling interval so that all curves could align.

Another Matlab script was made to recalculate the sampled points that were measured in Newton by the load cell to Newton meter, which is the unit of torque. This was done by multiplying the force with the lever, which gives torque.

3.4. Validation of Numerical Model

In order to make sure the numerical models are reliable they have to be validated. The validation of the numerical models is done using the results from the experimental setup. Each simulation has a correspondent experiment meaning that the inputs are the same e.g. rotational speed, type of oil, geometries etc. The output, or results, from the experiments are also the same as the output from the simulations, meaning that drag torque, oil flow characteristics and at which rotational speed oil enters the oil sump are the results in both the experimental setup and the simulations. Therefore, the numerical models will be quantitatively validated using drag torque and qualitatively validated using the oil flow characteristics and when the oil enters the oil sump.

3.4.1. Drag Torque

The procedure of the validation of drag torque will simply involve comparing of the collected data from the experiments and the data from the simulation. As the main focus of this thesis was to predict the drag torque in a wet clutch this validation segment is of great importance and if validated the main goal will be considered as reached.

3.4.2. Oil Flow Characteristics

As the numerical models are intended to be used in an optimization process in the future and thereby investigated in this thesis work it is important to analyze the oil flow characteristics of the numerical model. In order to optimize geometries in the wet clutch housing it is also important to know how it will affect the oil flow. The oil flow characteristics will be validated using the films from the high-speed camera and comparing them to the simulation. This will be done in different angles to ensure a broader validation.

3.4.3. Oil Entering the Oil Sump

This segment also applies to the optimization process as it is necessary to know at which rotational speed the oil starts to refill the oil sump. Also it is an easy way to measure in the experiments and then replicating it in the numerical models. The validation procedure for this segment will start from the experimental setup where the rotational speed at which the oil enters the oil sump is measured and then replicated using the numerical model. If, in the simulation, the oil enters the oil sump at a rotational speed close to that of the experiments, this segment will be considered as validated.

4. Results

The results from the experiments and from the numerical model will be presented in this paragraph. All torque data will be presented in the form of charts while the flow characteristic will be illustrated with images. A comparison between all the experiment, experimental data and the numerical model for different geometries and a mesh study will be presented.

4.1. Experimental Results

In Figure 4.1, Figure 4.2 and Figure 4.3 a summary of all experiments are shown. All the experiments have an oil immersion depth of 45mm and the main difference between these experiments are the inlet and outlet geometries. Figure 4.1 shows the results for an inlet of 2.5mm and outlet of 15mm, Figure 4.2 shows the results for an inlet of 10mm and outlet of 15mm and Figure 4.3 shows the results for an inlet of 10mm and outlet of 15mm and angle of 30 degrees which places the outlet later in the rotational direction of the drum. It is possible to see that the drag losses are lower when the inlet is smaller mainly because more oil is exiting through the outlet compared to what is entering through the narrow inlet. When it comes to Figure 4.3 it is hard to say if the losses are higher or lower than Figure 4.2 just by watching the figures and a more thorough investigation will be shown in section 4.5. Some experiments have results with zero losses, mainly regarding the speeds over 1000rpm and is due to a lot of vibrations at those speeds and is giving unreliable results.

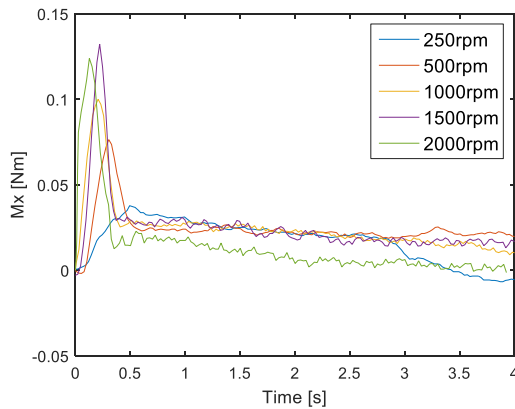


**Figure 4.1. Drag torque 250rpm-2000rpm
Inlet: 2.5mm, Outlet: 15mm, Angle: 0.**

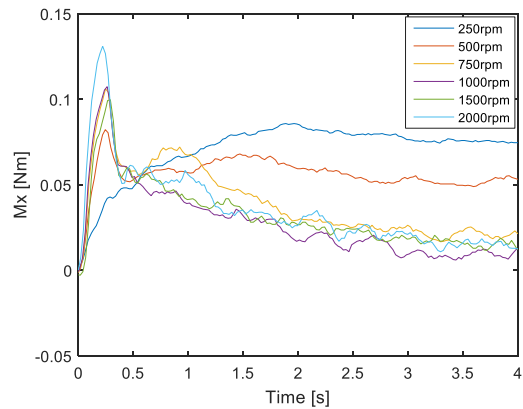


**Figure 4.2. Drag torque 250rpm-2000rpm,
Inlet: 10mm, Outlet: 15mm, Angle: 0.**

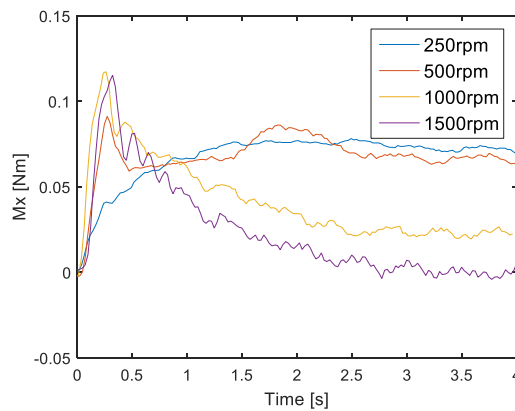
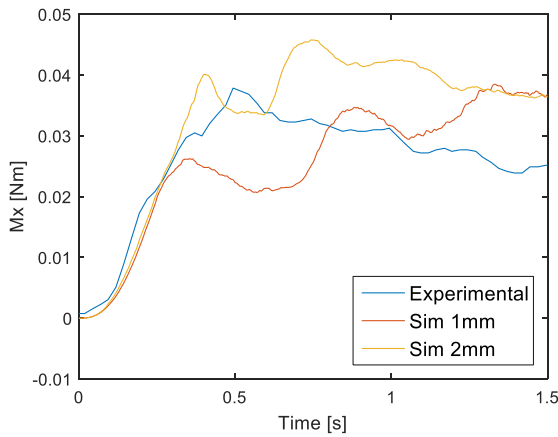


Figure 4.3. Drag torque 250rpm-1500rpm, Inlet: 10mm, Outlet: 15mm, Angle: 30.

4.2. Model Validation, 2.5 mm inlet

In Figure 4.4, Figure 4.5, Figure 4.6 and Figure 4.7 a comparison is shown between the experimental setup and the numerical model with different mesh sizes for an inlet of 2.5 mm and a rotational speed ranging from 250 rpm to 1500 rpm. In Figure 4.6 and Figure 4.7 the simulation time is shorter for the 1mm mesh size and this is because the simulation failed due to a memory error on the cluster. In all the figures it is possible to see the deviations between the experiments and the numerical model and this is mainly because the element size is too large for the numerical model and due to that the result is not reliable. There are still some similarities like the spike in the first 0.5 seconds which is during the ramp up phase and is very hard to capture.



**Figure 4.4. Drag torque at 250rpm
Inlet: 2.5mm, Outlet: 15mm.**

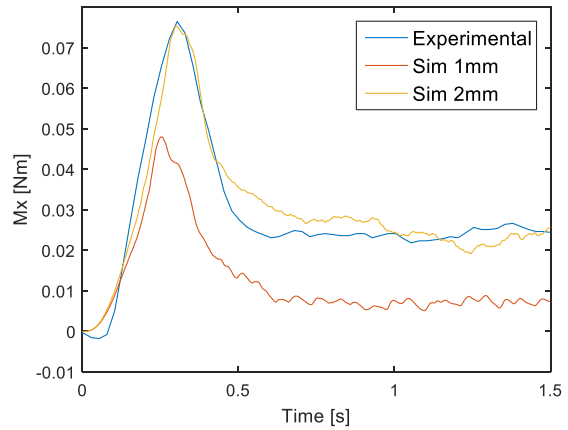


**Figure 4.5. Drag torque at 500rpm
Inlet: 2.5mm, Outlet: 15mm.**

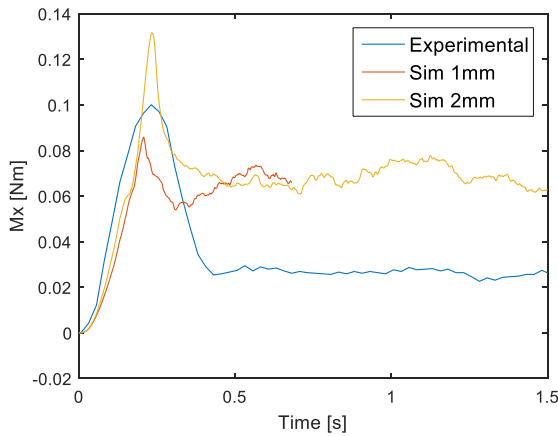


**Figure 4.6. Drag torque at 1000rpm
Inlet: 2.5mm, Outlet: 15mm.**

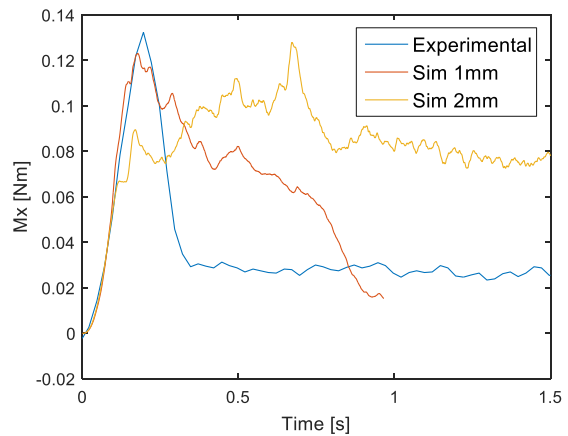


**Figure 4.7. Drag torque at 1500rpm
Inlet: 2.5mm, Outlet: 15mm.**

4.3. Model Validation, 10 mm inlet

In Figure 4.8, Figure 4.9, Figure 4.10 and Figure 4.11 a comparison is shown between the experimental setup and the numerical model with different mesh sizes for an inlet of 10 mm and an rpm range from 250 rpm to 1500 rpm. These results compared to the 2.5 mm inlet are more reliable due to the fact that the inlet here is 10mm and more elements can fit in the gap.

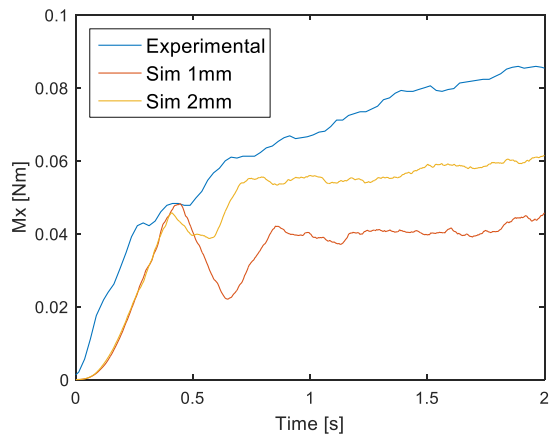


**Figure 4.8. Drag torque at 250rpm
Inlet: 10mm, Outlet: 15mm.**

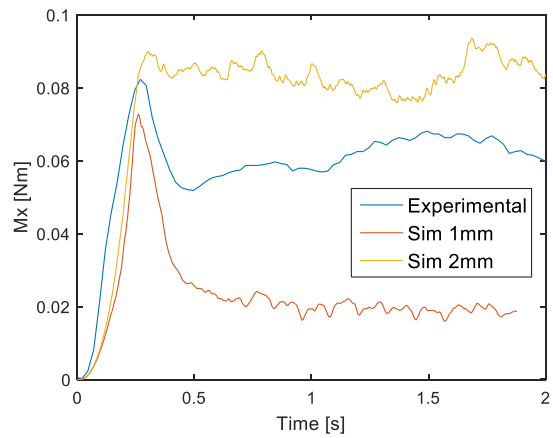


**Figure 4.9. Drag torque at 500rpm
Inlet: 10mm, Outlet: 15mm.**

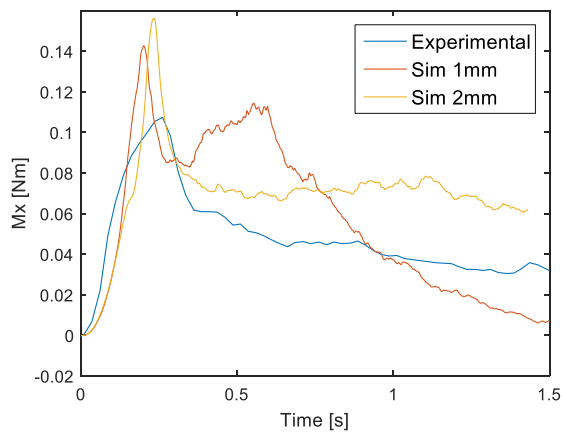


**Figure 4.10. Drag torque at 1000rpm
Inlet: 10mm, Outlet: 15mm.**

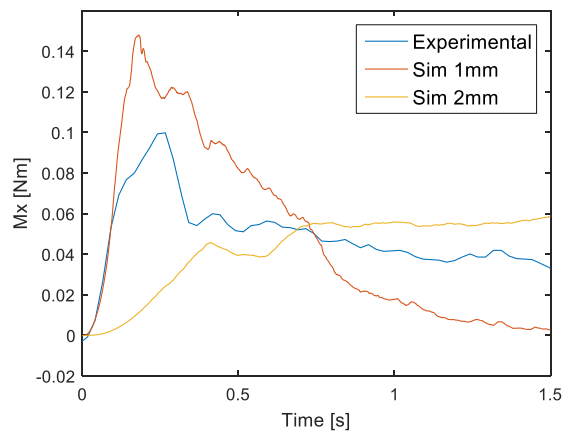


**Figure 4.11. Drag torque at 1500rpm
Inlet: 10mm, Outlet: 15mm.**

4.4. Mesh Study

A mesh study of the numerical model was conducted and the results are presented in Figure 4.12. The drag torque data presented was obtained by 500 rpm, inlet of 10mm, outlet of 15mm and three different mesh sizes. The results clearly show that the 2mm mesh is not suitable for the numerical model as the behavior of the drag torque does not match with the 1mm and 0.75mm mesh sizes.

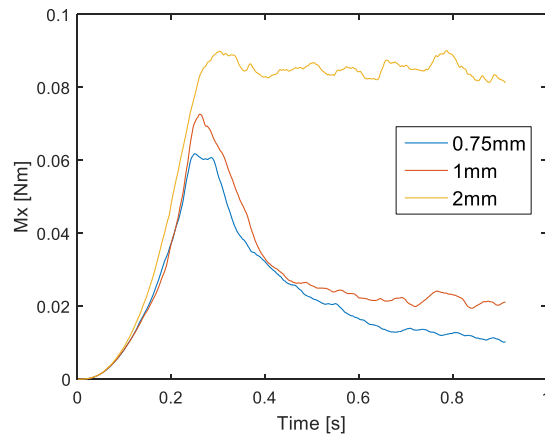


Figure 4.12. Drag torque at 500 rpm, Inlet: 10mm, Outlet: 15mm

4.5. Geometry Dependent Drag Torque Losses

Figure 4.13, Figure 4.14, Figure 4.15 and Figure 4.16 shows experimental data, where a more thorough investigation was done on how the torque losses are effected by positioning the outlet later in the rotational direction of the drum. In Figure 4.13 it is hard to distinguish the losses during the ramp up phase until after two seconds where it is shown that the losses are lower. This is due to the fact the fact that the 30-degree outlet actually throws out oil at 250 rpm while the 0 degree outlet dose not. In Figure 4.14 it is possible to see that the losses are higher when the angle is increased, in this case the rpm is increased to 500 rpm and both geometries throws out oil through the outlet and the same goes for Figure 4.15 where the rpm is increased to 1000 rpm. In Figure 4.16, when the rotational speed is increased to 1500 rpm, the values shift again and the losses gets lower for the 30 degree geometry. The data gathered for 1500 rpm is not reliable because it was impossible to distinguish the losses from the vibrations that was created by the system at any rotational speed over 1000 rpm.

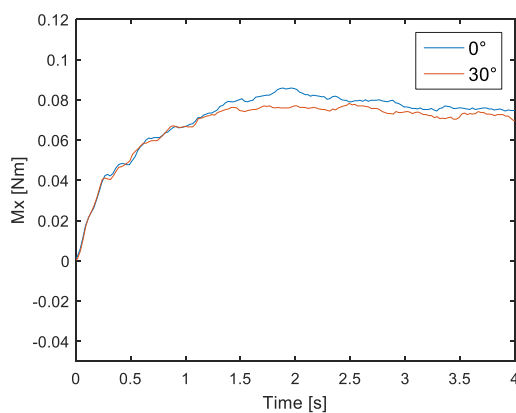


Figure 4.13. Drag torque at 250rpm with different angles.

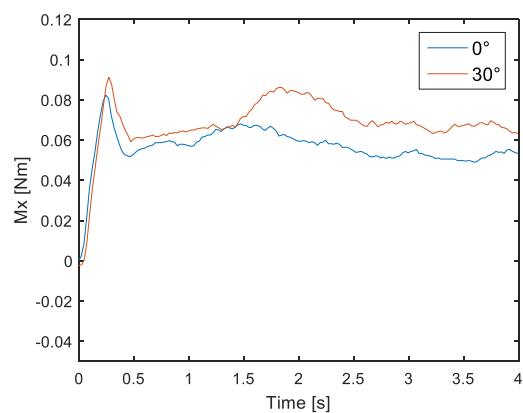


Figure 4.14. Drag torque at 500rpm with different angles.

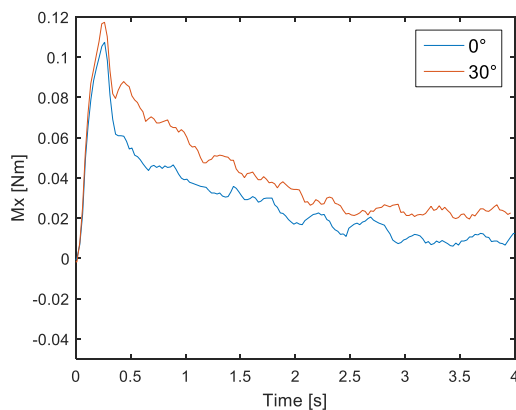


Figure 4.15. Drag torque at 1000rpm with different angles.

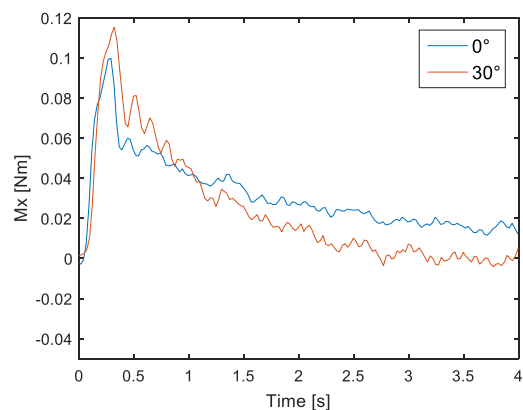


Figure 4.16. Drag torque at 1500rpm with different angles.

In Figure 4.17 the simulated results of a 2 mm mesh size are shown and it is possible to see how the torque is affected by the position change of the outlet in the numerical model when the rpm is set to 1000. The numerical model also shows that the losses get lower with an outlet that is earlier in the rotational direction of the drum. The different angles of the outlet geometry are defined as in Figure 3.12.

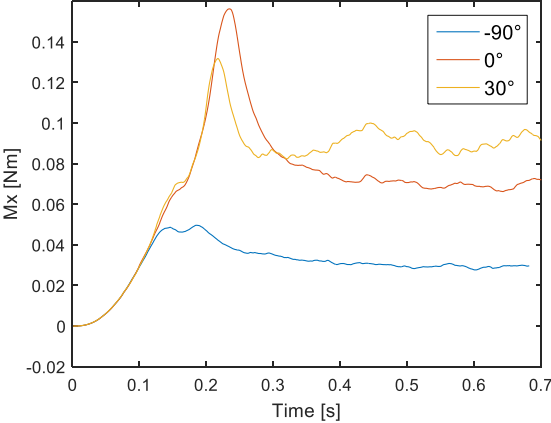


Figure 4.17. Simulated drag torque at 1000rpm with different outlet positions.

4.6. Oil Flow Characteristics

The results of the analysis of the oil flow characteristics is presented in this section. A pulsating behavior was captured both experimentally and numerically and are show in Figure 4.18 and Figure 4.19. Also a comparison, experimentally and numerically, between 250 rpm and 1000 rpm are shown in Figure 4.20 Figure 4.21, Figure 4.23 and Figure 4.24.

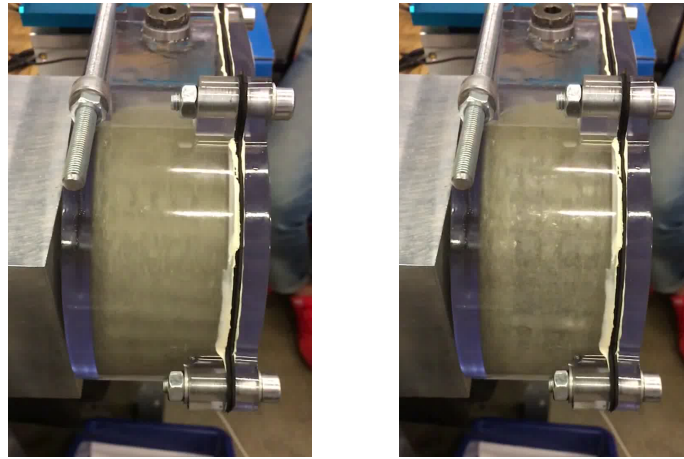


Figure 4.18. Experimental pulsating oil flow behavior, fully covered with oil (left), partly covered with oil (right).

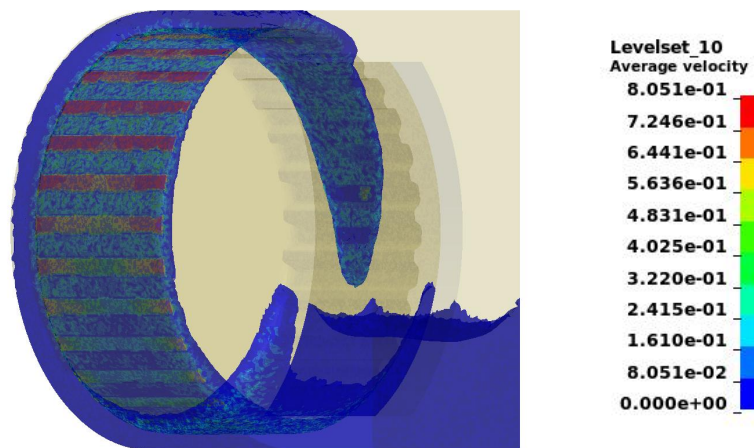


Figure 4.19. Simulated pulsating oil flow behavior seen by average velocity, 2 mm mesh size.

The pulsating oil flow behavior seen in Figure 4.18 correlates with the simulated pulsating oil flow behavior seen in Figure 4.19 where the coloring represents the average velocity of the oil. As the highest velocity only can be obtained by direct contact between the oil and the clutch drum it can be assumed that the red area represents oil that is in direct contact with the clutch drum. This phenomenon can also be seen experimentally where the clutch drum drags the oil in a pulsating motion and is thereby not in constant contact with the clutch drum. Sadly, it is hard to fully represent this result only using pictures.

Figure 4.20 and Figure 4.21 illustrates experimental and numerical results run at 250 rpm, 10mm inlet and 15mm outlet after 1.5 seconds with a mesh size of 2 mm. The purpose of this test was to show that the oil starts to flow into the oil sump at 250 rpm. Although the results do not show the oil entering the oil sump, in Figure 4.21, it definitely shows that the oil would have continued to flow into the oil sump. The reason it does not is due to the mesh size of 2mm being too large to represent such thin oil films. Another interesting behavior is the depletion of oil in the oil sump, approximately the same amount of oil has been dragged in through the inlet.



Figure 4.20. Experimental oil flow behavior after 1.5s at 250 rpm, 10mm inlet and 15mm outlet.

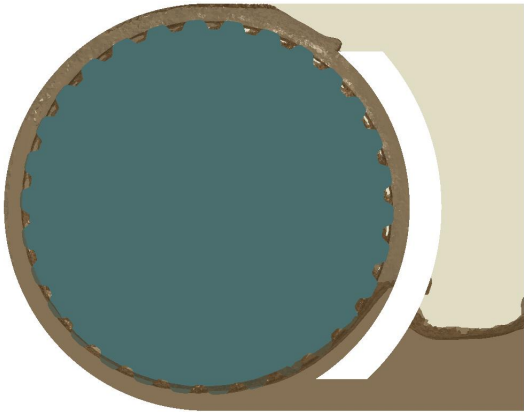


Figure 4.21. Numerical oil flow behavior after 1.5s at 250 rpm, 10mm inlet and 15mm outlet.

Figure 4.22, Figure 4.23 and Figure 4.24 illustrates experimental and numerical results run with 1000 rpm, 10mm inlet, 15mm outlet and a mesh size of 2 mm. The purpose of this test was to show where the oil hits the wall inside the oil sump and how well the oil timed the entering of the outlet.

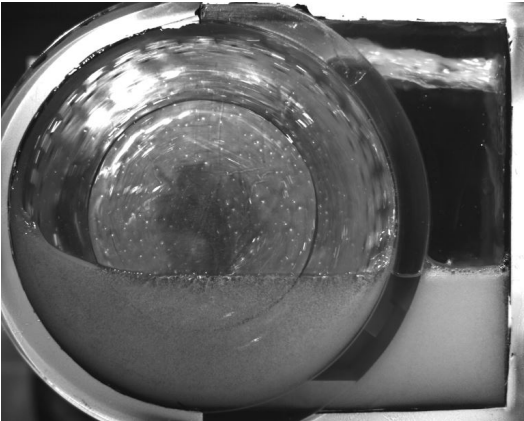


Figure 4.22. Experimental oil flow behavior after 0.09s at 1000 rpm, 10mm inlet and 15mm outlet.

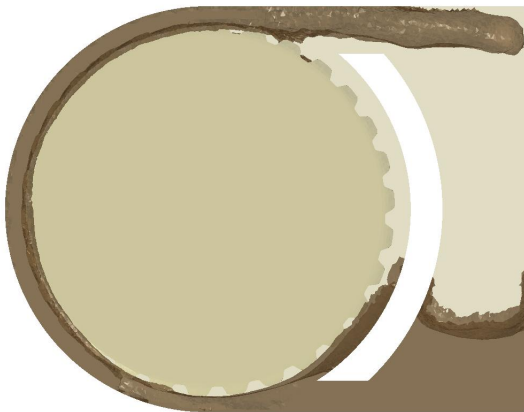


Figure 4.23. Numerical oil flow behavior after 0.36s at 1000 rpm, 10mm inlet and 15mm outlet.

As seen from Figure 4.22 and Figure 4.23 the time when the oil hits the inner wall of the oil sump does not correlate as the experimentally obtained time only elapsed 0.09 seconds and the numerically obtained time elapsed 0.36 seconds. The reason for this could be many, either the high-speed filming was off or there was

some sort of inertia in the numerical model. However, when it comes to comparing the experimental setup to the numerical model at the same elapsed time, Figure 4.23 and Figure 4.24, the oil inside the oil sump has decreased to about the same amount. Also it is possible to see oil between the clutch drum and cylinder wall just above the inlet, which is shown in Figure 4.24. This is the case for both the experimental setup and the numerical simulation.

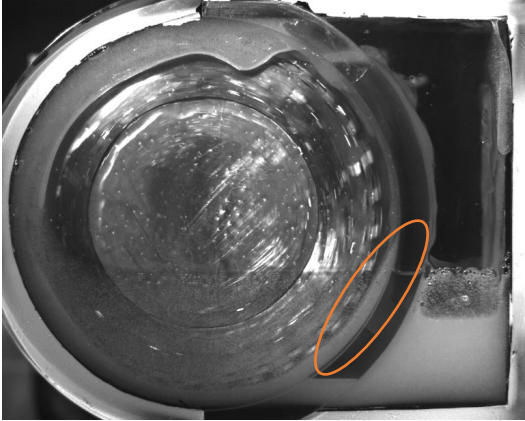


Figure 4.24. Experimental oil flow behavior after 0.36s at 1000 rpm, 10mm inlet and 15mm outlet.

5. Discussion

A discussion of the results will be presented in this paragraph and will be presented in the same order as the results are presented.

The 0.5mm mesh size was not presented in the results as the numerical simulations crashed due to memory errors on the cluster. This affected the mesh study, as it could have been done more thorough and a mesh convergence could have been calculated. Although, the other mesh sizes give a good insight of the behavior both when it comes to drag torque and oil flow characteristics.

The experimental setup had its limits due to vibrations in the system which made it difficult to measure drag torque above 1000 rpm. The load cell used for measuring the drag torque was sensitive and picked up vibrations in the system when exceeding 1000 rpm. However, some test runs were successful and the test procedure was thereby done by repeating the test until a successful test was accomplished. Although results from test with 1500 rpm are presented it is not reliable results and cannot determine the quality of the numerical model.

5.1. Experimental Setup

The experimental results show that the experimental setup is capable of measuring drag torque sufficiently well as the measured drag torque reacts to geometry changes as well as changes in rotational speed. However as mentioned above the vibrations in the system caused some problem when exceeding 1000 rpm. This can be seen in the results as the drag torque for the higher rotational speeds are not as smooth as for the lower rotational speeds. This can however easily be fixed by aligning and balancing the system properly.

5.2. Numerical Model vs. Experimental Setup

An overall comparison of the numerical model results and the experimental results shows that the numerical model clearly follows the behavior of the experimentally measured drag torque. The results however falter a bit when it comes to the tests done with an inlet of 2.5mm as the numerical model mesh size is not sufficiently small to represent the inlet with more than 2-3 elements in height. This causes problems when the oil travels from the oil sump through the inlet to the clutch drum. The results from the tests done with a 10mm inlet is thereby easier to simulate as the inlet can be represented by more elements and therefore gives more reliable results.

The 1mm mesh size show a much better approximation of the drag torque as it almost always lays below the experimentally measured drag torque. This has to be the case as the numerical model only takes drag torque losses from splashing in account, whereas the experimental tests have many more energy loss phenomenon. The only instances where the 1mm mesh size does not follow this behavior are at the test with 2.5mm inlet and 250 rpm and the test with 2.5mm inlet and 1000 rpm. The reason for the 250 rpm test being this way could be that the oil starts to enter the oil sump at 250 rpm and the amount of oil that enters through the inlet does not flow

through the outlet. This phenomenon can also be seen in the test with 250 rpm and an inlet of 10mm where the drag torque increases over time due to the increasing amount of oil surrounding the clutch drum.

5.3. Mesh Study

As mentioned in the beginning of the discussion the 0.5mm mesh size did not simulate very far as the cluster suffered from memory errors during the thesis. The mesh study is therefore only to show how the mesh size changes the results of the drag torque and not to determine mesh convergence. In the results from the mesh study it is clear that a finer mesh gives a lower drag torque, whether that is more correct cannot be said as the experimental setup needs to be isolated to only measure splash losses in order to determine this. A finer mesh however results in a longer simulation time and due to the memory errors on the cluster the longer simulation time only increased the risk of a memory crash. Although a finer mesh is more suitable to predict more reliable results when it comes to both drag torque and oil flow characteristics the 1mm and 2mm mesh shows the behavior of the two. The behavior is sufficient enough to be used in an optimization process where drag torque can be calculated for different geometries and compared to see which one give the least energy loss.

5.4. Geometry Dependent Drag Torque Losses

The drag torque losses are known to be dependent on geometry changes and this is clearly noticeable by the experimental setup. Simply by positioning the outlet 30 degrees later in the rotational direction the drag torque increased. As seen from the results the drag torque did not increase for every test scenario but there is an explanation for this. At 250 rpm the oil barely flows over to the oil sump when it comes to the 0-degree, 15mm outlet, the oil simply does not have the energy to be thrown over to the oil sump. But when it comes to the 30-degree outlet the oil has a longer projectile and will therefore escape through the outlet easier. This means that the amount of oil surrounding the clutch drum is smaller when running the test with a 30-degree outlet compared to the 0-degree outlet. Also the drag torque did not increase at 1500 rpm and this has to do with the vibrations in the system.

The results from the geometry analysis done on the numerical model also show that the 30-degree outlet gives a higher drag torque than a 0-degree outlet. For comparison a simulation of a negative 90-degree outlet was conducted and it clearly shows that the drag torque can be lowered even further. The reason for this phenomena is that by positioning the outlet earlier in the rotational direction the oil can escape much quicker and the splash losses thereby decreases. The main reason for not placing the outlet in this position is due to difficulties in designing the oil sump to be connected to the outlet and inlet when they are placed too far from each other.

5.5. Oil Flow Characteristics

The behavior of the flow is very hard to capture in a numerical model, with that being said the data collected both experimentally and numerically show some interesting results. The results between the tests and simulations clearly shows that the oil level inside the oil sump decreases roughly at the same pace and is not

affected by the rotational speed. It has also been shown that the rotational speed at which the oil starts to enter the oil sump through the outlet is 250 rpm both experimentally and numerically.

An interesting phenomenon was the pulsating behavior of the oil surrounding the clutch drum. This behavior was found both experimentally and numerically. A possible explanation for this is that the oil cumulates to a point at which the clutch drum can grab onto the oil and drag it around the cylinder. When this happens the oil spreads out until it cumulates again and the process repeats itself and a pulsating behavior is obtained.

6. Conclusions

The conclusions of this thesis is that numerical models can predict drag losses and oil flow characteristics to a certain degree but can be used for optimization purposes. The numerical model used in this thesis will predict drag loss changes for different geometries of the clutch housing and can therefore be used as an optimization tool in making the wet clutch more efficient. However, the results do not predict the exact drag loss for a wet clutch system as it only takes splash losses into account. The experimental setup was able to measure small geometry changes which correlates to the simulated geometry change when it comes to the behavior of the drag torque.

The oil flow behavior on the drum showed promising results as the experimentally obtained rotational speed for oil starting to enter the oil sump correlated with the simulated rotational speed. Also the pulsating oil flow behavior, even though it does not contribute to any specific feature of a wet clutch, was captured both experimentally and numerically and correlated with one and other. The position at which the oil hits the inner wall of the oil sump at 1000 rpm also correlated between the experimental setup and the numerical model, although the elapsed time differed. The oil level inside the oil sump also correlated between the experimental setup and the numerical model as the oil level decreased at the same pace. All of these confirmations implies that even the oil flow characteristics of the numerical model can be predicted and used for optimization purposes.

Although most of the results show the potential of using numerical models for predicting drag torque and oil flow characteristics it still needs to be developed further for industrial purposes. Many problems in the numerical model comes down to hardware and software. LS-DYNA has come very far when it comes to these types of simulations, but it still needs to be developed further in order to simplify the models and making them numerically stable. The smaller mesh sizes result in very long simulation times that could be minimized if a model without FSI could be made. A model without FSI would also run solely on the incompressible fluid dynamics solver where an implicit solver always is used. This would result in more reliable results as the results only comes from one solver.

7. Future work

As the numerical model classifies as a second generation simulation model it still needs additional work in order to be used as an optimization tool when designing wet clutch systems. Mainly it is dependent on what LS-DYNA is capable of and how it will be developed in the future. Here are some recommendations on future work in order to further develop the numerical model:

- Making the numerical model more stable by conducting a more thorough mesh study
- Making a numerical model without FSI coupling i.e. ICFD solver only
- Simulate until steady-state has been reached
- Model the air as air instead of void
- Making the 2D-model numerically stable
- Simulate a real wet clutch system for comparison
- Investigate the ICFD-MATERIAL card and different oils in order to see its influence

Here some recommendations follow on future work for the test setup to achieve a more controlled testing environment:

- Reduce vibrations in the system by a better alignment of the electric motor and the clutch drum shaft
- Using a custom made clutch drum designed specifically to the test setup
- Analyze how much energy loss that dissipates due to the bearings holding the clutch housing

Finally, some future work that would be of interest to further develop the project:

- Conducting a more thorough investigation of the oil flow characteristics in order to specify different behaviors to compare, both experimentally and numerically
- Inserting lamellae to the clutch system, both experimentally and numerically
- Introduce thermal effects to the system, both experimentally and numerically

8. References

- [1] R. Nibumolu, C. Prahalad and M. Ranganaswami, "Why Sustainability Is Now the Key Driver of Innovation," *Harvard Business Review*, September 2009.
- [2] K. Holmberg, P. Andersson and A. Erdemir, "Global energy consumption due to friction in passenger cars," *Tribology International*, no. 47, pp. 221-234, 2012.
- [3] Y. Takagi, H. Nakata, Y. Okano, M. Miyagawa and N. Katayama, "Effect of Two-phase Flow on Drag Torque in a Wet Clutch," *Journal of Advanced Research in Physics*, vol. 2, no. 2, pp. 1-5, 2011.
- [4] S. Iqbal, F. Al-Bender, B. Pluymers and W. Desmet, "Model for Prediction Drag Torque in Open Multi-Disks Wet Clutches," *Journal of Fluids Engineering*, vol. 136, pp. 1-11, 2014.
- [5] R. Mäki, B. Ganemi, E. Höglund and R. Olsson, "Wet clutch transmission fluid for AWD differentials: influence of lubricant additives on friction characteristics," *Lubrication Science*, vol. 19, pp. 87-99, 2006.
- [6] B. PDS, "Presentation of the product line up," Landskrona, 2016.
- [7] C. Changenet and P. Velex, "Housing influence on churning losses in geared transmissions.," *Journal of Mechanical Design*, vol. 130, no. 6, pp. 1-6, 2008.
- [8] K. A. Gardner, J. D. Seidt and A. Gilat, "Validation FSI Simulations in LS-DYNA 971 R7.," *Experimentat and Applied Mechanics*, vol. 6, pp. 55-58, 2015.
- [9] E. Nyberg and J. Hansen, "Fluid Structure Interaction in Wet Clutch Systems," Luleå University of Technology, Luleå, 2015.
- [10] M. Johansson and E. Söderström, "Prediction of oil flow and drag torque losses in wet clutch systems," Luleå University of Technology, Luleå, 2016.
- [11] Q. J. Wang and Y.-W. Chung, "Encyclopedia of Tribology," in *Encyclopedia of Tribology*, New York, Springer, 2013, pp. 3816-3818.
- [12] B.-R. Höhn, K. Michaelis and H.-P. Otto, "Influence of immersion depth of dip lubricated gears on power loss, bulk temperature and scuffing load carrying capacity," *International Journal of Mechanics and Materials in Design*, vol. IV, no. 2, pp. 145-156, June 2008.
- [13] K. Al-Shibl, K. Simmons and C. N. Eastwick, "Modelling windage power loss from an enclosed spur gear.," *Proceedings of the Institution of Mechanical Engineers, Part A: Journal of Power and Energy*, vol. 221, no. 3, pp. 331-341, 2007.
- [14] R. P. Rodrigo, "Incompressible fluid solver," Livermore Software Technology Coporation, 2014.
- [15] P. Jonsen, "Large deformation analysis M7009T," in *Luleå University of Technology*, Luleå, 2016.
- [16] "Altair University," [Online]. Available: http://www.altairuniversity.com/wp-content/uploads/2012/04/Student_Guide_211-233.pdf. [Accessed 14 Juni 2016].
- [17] I. Dehli, "Multi disk friction clutch," NPTEL, 2012. [Online]. Available: <http://nptel.ac.in/courses/116102012/106>. [Accessed 21 April 2016].

9. Appendix

Table of Contents

A. Deep groove ball bearing, single row, SKF 6008-2Z	I
B. Y-bearing plummer block unit, SKF SY 15 TF	II
C. Material data for Accura ClearVue	III
D. Comparison between 0° outlet and 30° outlet	IV
E. Structural analysis of test setup	V
E.1. Structural analysis of clutch drum shaft	V
E.2. Structural analysis of wet clutch housing	VI

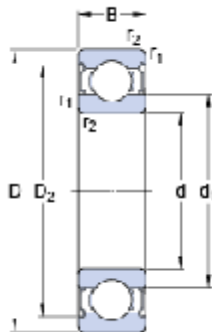
A. Deep groove ball bearing, single row, SKF 6008-2Z



6008-2Z

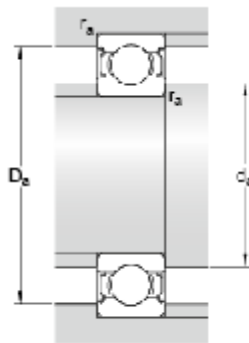
SKF Explorer

Dimensions



d		40	mm
D		68	mm
B		15	mm
d ₁	≈	49.25	mm
D ₂	≈	61.1	mm
r _{1,2}	min.	1	mm

Abutment dimensions



d _a	min.	44.6	mm
d _a	max.	49.2	mm
D _a	max.	63.4	mm
r _a	max.	1	mm

Calculation data

Basic dynamic load rating	C	17.8	kN
Basic static load rating	C ₀	11	kN
Fatigue load limit	P _u	0.49	kN
Reference speed		22000	r/min
Limiting speed		11000	r/min
Calculation factor	k _r	0.025	
Calculation factor	f ₀	15	

Mass

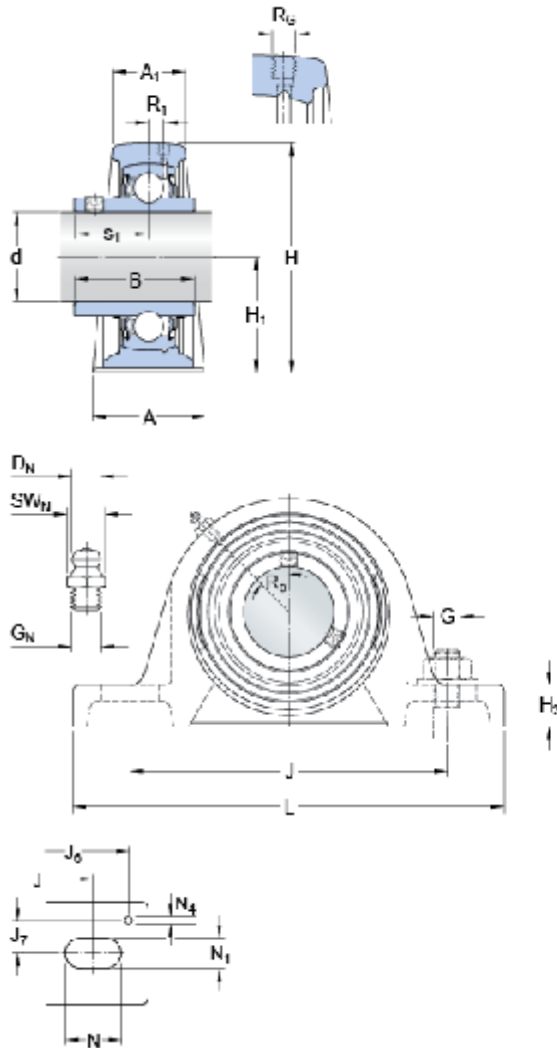
Mass bearing		0.201	kg
--------------	--	-------	----

B. Y-bearing plummer block unit, SKF SY 15 TF



SY 15 TF

Dimensions



d	15	mm
A	32	mm
A ₁	18	mm
B	27.4	mm
H	57	mm
H ₁	30.2	mm
H ₂	14	mm
J	97	mm
J max.	106	mm
J min.	88	mm
L	127	mm
N	20.5	mm
N ₁	11.5	mm
s ₁	15.9	mm

Threaded hole

R _G	1/4-28 UNF	
R ₁	1	mm
R ₀	45	°

Grease fitting

D _N	6.5	mm
SW _N	7	mm
G _N	1/4-28 SAE-LT	

Dowel pins

J ₆	118	mm
J ₇	11.5	mm
N ₄	2	mm

C. Material data for Accura ClearVue

Table C.1. Material properties for Accura ClearVue.

Properties	Accura[®] ClearVue
Material color	Not colored (transparent)
Special properties	Similar to ABS strong, flexible, biodegradable
Hardness (shore A/D 23°C)	-
Flexural Modulus (MPa)	1980-2310
Flexural Strength (MPa)	72-84
Young's Modulus (MPa)	2270-2640
Tensile Strength (MPa)	46-53
Heat Deflection Temp °C (HDT) *) 66 PSI	51
Glass transition Temp °C (Tg)	62
Elongation at Break (%)	3-15
Izod Impact (kJ/m ²) * Notched J/m	40-58*

D. Comparison between 0° outlet and 30° outlet

In Figure D.1 and Figure D.2 below a comparison between a 0-degree outlet and a 30-degree outlet is shown.

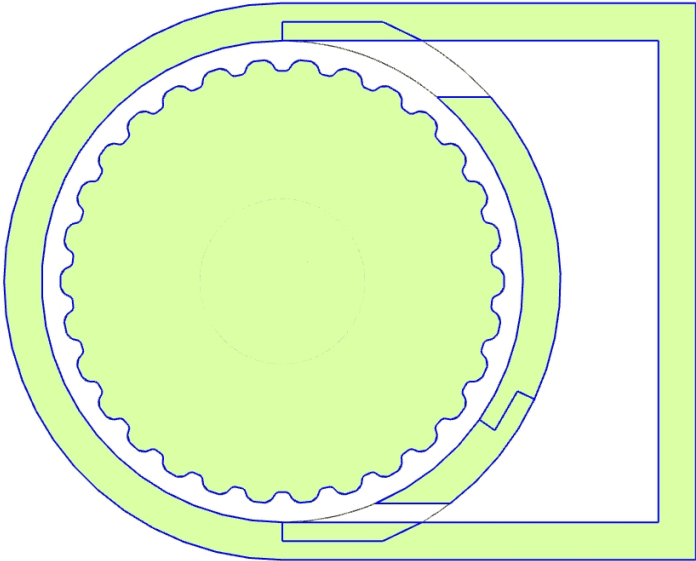


Figure D.1. Section view of wet clutch housing with 0-degree outlet.

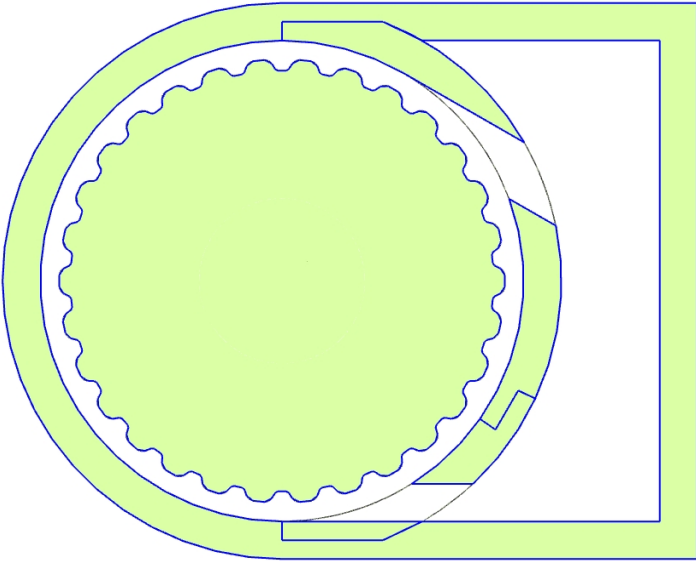


Figure D.2. Section view of wet clutch housing with 30-degree outlet.

E. Structural analysis of test setup
E.1. Structural analysis of clutch drum shaft

Table E.1. Material properties of steel from Siemens NX material library.

Properties	Steel
Mass Density (kg/mm ³)	7.829e-6
Young's Modulus (MPa)	206940
Tensile Strength (MPa)	276
Yield Strength (MPa)	137.895
Poisson's Ratio	0.288

The results clearly show that there is no problem at all when it comes to the clutch drum shaft being in contact with the wet clutch housing as the shaft only displaces 0.1101 mm and that is at the very end where the clutch drum is supposed to be mounted. The results are shown in Figure E.1 below.

axel_sim2 : Solution 1 Result
 Subcase - Static Loads 1, Static Step 1
 Displacement - Nodal, Magnitude
 Min : 0.0000, Max : 0.1101, Units = mm
 Deformation : Displacement - Nodal Magnitude

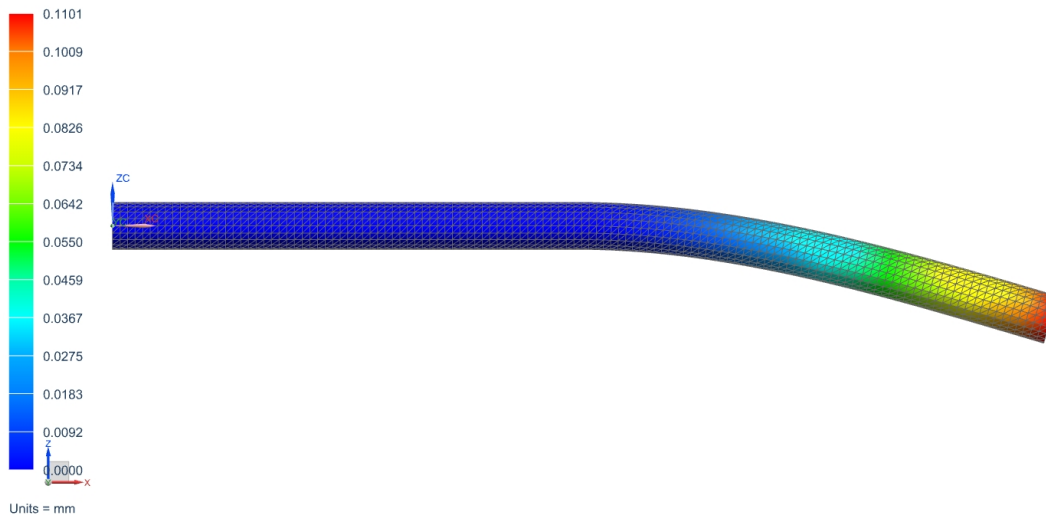


Figure E.1. Results of the structural analysis on the clutch drum shaft.

E.2. Structural analysis of wet clutch housing

Table E.2. Material properties of acrylic from Siemens NX material library.

Properties	Acrylic
Mass Density (kg/mm ³)	1.2e-6
Young's Modulus (MPa)	2000
Yield Strength (MPa)	48
Poisson's Ratio	0.4

The results from the structural analysis on the wet clutch housing can be seen in Figure E.2 below. It is clearly shown that it would be no problem at all using the Accura ClearVue Material as that material is stronger than the chosen material for this structural analysis. The results show a displacement of 0.157 mm at the very end of the wet clutch housing, which would be no problem.

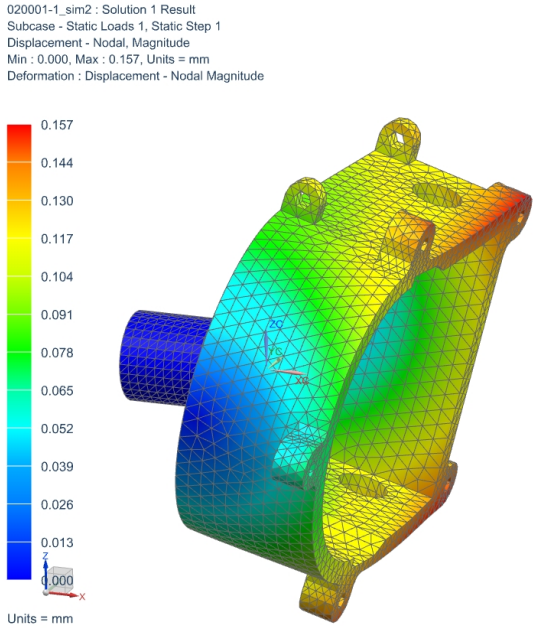


Figure E.2. Results from the structural analysis of the wet clutch housing.